Robert McIntosh
Director, Product Safety
Commercial Airplanes

The Boeing Company
P.O. Box 3707 MC 084-61
Seattle, WA 98124-2207

BOEING

15 September, 2022
66-CB-H200-ASI-19270

Sathya Silva
National Transportation Safety Board
490 L' Enfant Plaza East, SW
Washington, DC 20594

Subject: Boeing Component Examination Report - Red Air MD-82 HI1064 Landing Gear Collapse and Runway Excursion Miami, Florida - 21 June, 2022

Dear Ms. Silva:

In support of the US NTSB investigation into the subject event, Boeing's Huntington Beach Laboratory was asked by the NTSB to perform an examination of the Left Main Landing Gear recovered from the subject airplane. Please find the Component Examination Report enclosed with this letter.

The information included with this correspondence is controlled under the US Export Administration Regulations (15 CFR Parts 300-799) and has been categorized as ECCN: 9E991.

Please feel free to contact us if you have any questions.

Best regards,

[redacted]

Robert J. McIntosh
Director, Product Safety

Enclosure: Boeing Component Examination Report - Red Air MD-82 HI1064 Landing Gear Collapse and Runway Excursion Miami, Florida - 21 June, 2022

Engineering Report No: MS 80040

To: [redacted]

CC:

EXPORT CONTROLLED - This technology or software is subject to the U.S. Export Administration Regulations (EAR), (15 C.F.R. Parts 730-774). No authorization from the U.S. Department of Commerce is required for export, re-export, in-country transfer, or access EXCEPT to country group E:1 or E:2 countries/persons per Supp.1 to Part 740 of the EAR.

FRACTURE ANALYSIS REPORT

Engineering Report No: MS 80040 **Date: 8/15/2022**

Lab BLIS Number(s): 028-2022-07-12-00527

Part Information:

Design Drawing Part Names, Part Numbers, and Serial Numbers:

- Strut Assy, MLG, P/N 5935355-501 (S/N CPT0718)
- Torque Arm, Upper MLG, P/N 5935374-5 (S/N MAL112)
- Torque Arm, Lower MLG, P/N 5935353-5 (S/N MAL294)
- Link – Upper Side Brace, MLG, P/N 5935346-503 (S/N AEC284)
- Link – Lower Side Brace, MLG, P/N 5935351-9 (S/N CET0492 MHB)
- Rod, Retract Cylinder, MLG, P/N 5937036 (S/N unknown)
- Link, Upper Lock, P/N 5935349-9 (S/N AML0050)
- Link, Lower Lock, P/N 5935350-7 (S/N CPT0893MHB)
- Piston Rod – Bungee Cylinder / P/N 5937035-1/ (Assy S/N CPT0852)
- Shimmy Damper Assy, P/N SR09320057-7009 (S/N DL84)
- Bolt – Apex, Torque Link, P/N 4925624-501 (S/N CPT979)

Responsible Design Group: Landing Gear

Airplane Information:

A/P Customer:	RedAir	A/P Model:	MD-82
Registry No:	HI1064	Line Position No:	1805
Flight Hours:	68,229	Number of Landings:	35,873

Material Information:

Material / Heat Treat / Material Specification

Torque Arms -	300M Steel / 275-305 ksi per DPS 5.00 / DMS 1935
Side Brace Links -	300M Steel / 275-305 ksi per DPS 5.00 / DMS 1935
Retract Rod -	4340 Steel / 180-200 ksi per DPS 5.00 / MIL-S-5000 Cond E1
Lock Links -	Hy-Tuf / 220-240 ksi per DPS 5.00/ DMS 1841
Bungee Piston -	17-4 PH CRES / H900 per DPS 5.00 / AMS 5643
Apex Bolt -	4340 Steel / 180-200 ksi per DPS 5.00 / MIL-S-5000

Finish:

Torque Arms* - Cadmium Plate per DPS 9.28
Side Brace Links* - Cadmium Plate per DPS 9.28
Retract Rod - Chromium Plate per DPS 9.71
Lock Links* - Cadmium Plate per DPS 9.28
Bungee Piston* - Hard Chromium plate per DPS 9.71
Apex Bolt* - Cadmium Plate per DPS 9.28

*Impact Resistant Primer, DMS2144 and Gray Impact Resistant Polyurethane Topcoat, DMS2143 DN3635 per DPS4.50-62.

SUBJECT: Fractographic Evaluation: MD-82 Left Main Landing Gear Strut Assembly

BACKGROUND:

On 21 June 2022, a Red Air MD-82, registration HI1064, on flight L5203 experienced a runway excursion and gear collapse during landing on runway 09 at Miami International Airport. Initial reports indicated that the left main landing gear collapsed prior to the excursion, and the aircraft subsequently came to rest left of the runway with a fire developing on the right wing after contacting ground equipment. Emergency services extinguished the fire, and all passengers evacuated via left slides and wing with minor injuries reported to four occupants.

The event airplane (Effectivity 80J213, L/N 1805, S/N 53027) was delivered to another operator in December 1990. At last report (04/30/2018), the airplane had accumulated 35,873 cycles and 68,229 flight hours.

The left MLG shock strut assembly was subsequently sent to Boeing BR&T Laboratories in Huntington Beach, CA for evaluation in coordination with the NTSB and FAA (Figures 1 to 4).

EXPERIMENTATION AND RESULTS:

Torque Arms and Apex Bolt

Macroscopic Examination

The lower torque arm was still attached to the axle, and the upper torque arm was still attached to the cylinder in the as-received condition (Figure 3). The lower torque arm exhibited two complete, transverse fractures which intersected the upper lug hole, approximately 1.6 inches from the end of the part (Figures 5 to 7). Both of the fracture halves closest to the upper end were relatively smooth and smeared in an inboard/outboard direction (Figure 6). The fracture surfaces occurred along an oval/elliptical path, indicating that the fracture may have occurred due to a combination of compression and bending/shearing. The mating fracture halves were heavily damaged due to post-fracture smearing (Figure 7). The fractured lug end appeared to be bent slightly in an inboard direction.

The upper torque arm exhibited transverse fractures through one of the shimmy damper attachment lugs (Figures 5 and 8 to 10). The fractures intersected almost diametrically opposite sides of the attachment lug hole. A large portion of one of the fractures was obscured. Undamaged regions were smooth in texture and smeared, typical of shear. The fractured area at the outer end of the lug was twisted in an inboard direction (Figure 10).

The associated apex bolt was difficult to remove from the assembly (Figure 9). Once removed, it was observed that the bolt was slightly bent.

Scanning Electron Microscopy (SEM)

SEM analysis of the fracture surfaces in the lower torque arm revealed evidence of ductile separation (Figures 11 to 23). The upper and lower fracture surfaces of the lower torque arm exhibited a mixture of shallow elongated dimples, typical of shear, and somewhat more equiaxed dimples, typical of bending. Shear dimples were open toward the outboard side, suggesting that the fracture propagated in an inboard direction relative to the remainder of the part during fracture. SEM analysis revealed that the mating fracture halves were obliterated by post-fracture mechanical damage.

Energy Dispersive Spectroscopy (EDS)

EDS analysis of the smeared fracture of the lower torque arm half revealed the presence of aluminum, nickel, and iron oxide (Figures 24 to 27). Aluminum may have resulted from impact with the shimmy damper housing; nickel was most likely smeared from the nickel-plated lug hole; and iron oxide was due to post-fracture oxidation [rust].

EDS analysis indicated that the base material of the lower torque arm was consistent with the chemistry of DMS 1935 for 300M steel (Table I).

Hardness

Hardness measurements from the lower torque arm resulted in an average value of HRC 54.4 which was within the range of HRC 53 to 55 specified by DPS 1.05-4 for 300M steel heat treated to a UTS of 275 to 305 ksi. Hardness measurements from the bent apex bolt resulted in an average value of HRC 40.7 which was within the range of HRC 40 to 43 specified by DPS 1.05-4 for low alloy steel heat treated to an ultimate tensile strength of 180 to 200 ksi.

Side Brace Links

Macroscopic Examination

Note: for discussion purposes, all orientations depicted in this report for the side braces are with the side braces in the normal, extended position (LG deployed position).

The lower side brace link was still attached to the shock strut cylinder in the as-received condition (Figure 3). The upper side brace link had been separated from the assembly. Once reassembled, witness marks on the cylinder and links indicated that the side brace assembly had become hyper-extended and crossed over the cylinder (transitioned from inboard to outboard side of cylinder) during the incident (Figures 28 to 31).

The upper side brace link exhibited two complete, transverse fractures which were located approximately 10 inches and 15 inches from the lower end (Figures 32 and 33). Both fractures initiated from areas of mechanical damage along the aft, outboard flange. The fractures were arbitrarily identified as #1 and #2 in the lab for discussion purposes. The origin area of fracture #1 was heavily smeared (Figure 34). The flange was heavily damaged and deformed inward in this area. The origin area of fracture #2 exhibited an elliptical shape, and the fracture surface exhibited a dull texture, typical of ductile separation (Figure

35). During sectioning in the lab, a secondary crack which intersected fracture #1 was exposed (Figures 33 and 36). The initial portion of this crack, which originated from fracture #1, exhibited a somewhat grainy texture, typical of brittle fracture, to a crack depth of 0.09 inch (Figure 37). This initial portion did not appear oxidized.

The lower side brace link exhibited a complete, transverse fracture approximately 4.1 inches from the upper end (Figure 38). The fracture initiated at the forward, inboard flange (Figure 39). The origin area appeared elliptically-shaped and rusted to a crack depth of 0.05 inch (Figure 40). The remainder of the fracture surface appeared less oxidized and exhibited a dull texture, typical of ductile separation. Witness/damage marks along both sides of the fracture indicated that the pieces were still together during hyper-extension of the side brace links (Figure 38).

Scanning Electron Microscopy (SEM)

A majority of the origin area of fracture #1 in the upper side brace link was smeared from post fracture damage. All undamaged, observable regions exhibited evidence of ductile separation (Figures 41 to 46).

SEM analysis of the secondary crack which intersected fracture 1 revealed a mixture of intergranular, quasi-cleavage, and dimpled morphology to a crack depth of 0.09 inch (Figures 47 to 51). Beyond this depth, the remainder of the crack exhibited evidence of ductile separation (Figure 52).

SEM analysis of fracture #2 revealed evidence of ductile separation (Figures 53 to 57).

SEM analysis of the lower side brace link revealed evidence of intergranular separation to a crack depth of 0.05 inch (Figures 58 to 62). This region appeared oxidized. The remainder of the fracture exhibited evidence of ductile separation (Figure 63).

Energy Dispersive Spectroscopy (EDS)

EDS analysis indicated that the base materials of both side brace links were consistent with the compositional requirements of DMS 1935 for 300M steel (Table II).

Hardness

Hardness measurements from the side brace links resulted in average values of HRC 54.8 [upper link] and HRC 54.7 [lower link] which were within the required range of HRC 53 to 55 specified by DPS 1.05-4 for 300M steel heat treated to a UTS of 275 to 305 ksi.

Retract Cylinder Rod

Macroscopic Examination

The retract cylinder rod was still attached to the cylinder in the as-received condition (Figure 3). The rod exhibited a complete, circumferential fracture approximately 16 inches from the attached end (Figure 64). The rod was bent in an outboard direction. The fracture surface occurred along oblique planes and the fracture end portion, along the concave side, was locally buckled, typical of ductile separation due to bending (Figure 65).

Scanning Electron Microscopy (SEM)

SEM analysis of the fracture surface revealed evidence of ductile separation (Figures 66 to 73).

Energy Dispersive Spectroscopy (EDS)

EDS analysis indicated that the base material of the retract rod met the requirements of MIL-S-5000 for 4340 steel (Table III).

Hardness

Hardness measurements from the retract rod resulted in an average value of HRC 40.2 which was within the required range of HRC 40 to 43 specified by DPS 1.05-4 for low alloy steel heat treated to a UTS of 180 to 200 ksi.

Lock Links

Macroscopic Examination

Note: for consistency, all orientations depicted in this report for the lock links are relative to the side braces in the extended position (LG deployed position).

The lower lock link exhibited complete transverse fractures through the arm approximately four inches from the inboard end (Figures 74 to 78). The upper end of the lower link was still attached to the upper link (Figures 74 and 75), and the lower end (the lug portion of lower lock link) was still attached to the side braces in the as-received condition (Figure 76). The lower lock link was bent in an upward and aft direction (Figures 77 and 78). The upper link was bent in a forward direction (Figure 77). One fracture intersected a hole in the arm (Figures 79 and 80). This fracture consisted of two segments which intersected diametrically opposite sides of the hole. The fracture surfaces were smeared in a forward/aft direction (Figure 80). The other fracture appeared to have occurred outside the hole (Figure 81). This fracture appeared smeared in a longitudinal (up/down) direction.

Scanning Electron Microscopy (SEM)

SEM analysis of each fracture surface revealed evidence of ductile separation. A majority of dimple formations were shallow and stretched, typical of ductile separation due to shear loads (Figures 82 to 91).

Energy Dispersive Spectroscopy (EDS)

EDS analysis of the lower lock link indicated that the base material was consistent with the compositional requirements of DMS 1841 for Hy-Tuf steel (Table IV). EDS analysis was not performed on the upper lock link.

Hardness

Hardness measurements from the lower lock link resulted in an average value of HRC 49.4 which was slightly higher than the range of HRC 46 to 49 specified by DPS 1.05-4 for Hy-Tuf steel heat treated to a UTS of 220 to 240 ksi.

Bungee Piston Rod

Macroscopic Examination

The bungee piston rod exhibited a complete fracture approximately two inches from the end of the clevis lug (Figures 92 to 94). The fracture surface occurred along an oblique plane, typical of ductile separation (Figures 95 and 96). The rod appeared to be bent slightly in an aft direction in the area of fracture.

Scanning Electron Microscopy (SEM) and Energy Dispersive Spectrometry (EDS) Analysis

SEM analysis of the fracture surface revealed evidence of ductile separation (Figures 97 to 101).

Energy Dispersive Spectroscopy

EDS analysis indicated that the base material of the bungee piston rod was consistent with the compositional requirements of AMS 5643 for 17-4 PH CRES (Table V).

Hardness

Hardness measurements from the bungee rod resulted in an average value of HRC 44.5 which was within the range of HRC 40 to 47 specified by DPS 1.05-5 for 17-4 PH CRES heat treated to a H900 condition.

Shimmy Damper

Macroscopic Examination

The shimmy damper housing exhibited evidence of impact damage, and a number of the threaded inserts had partially pulled out of the housing (Figure 102). Some of the insert threads contained remnants of the mating shimmy damper housing threads which had been sheared away. The ends of the holes were elongated in a mostly circumferential direction (Figure 103). The hole surfaces exhibited circumferential scrape/shear marks (Figure 104).

The shimmy damper was requested to be returned intact which precluded performing any SEM analysis, nor hardness or chemical analysis for alloy verification by Boeing.

Shock Strut Fluid

A sample of hydraulic fluid was collected from the shock strut at the incident site. Fourier-transform infrared spectroscopy (FTIR) analysis identified the fluid as DPM 6176, MIL-PRF-5606 hydraulic fluid (See Appendix 1). Acidity was measured to be 3.59 mg KOH/g, which met the requirement of 2.3 to 5.0 mg KOH/g specified by MIL-PRF-5606. Moisture content was above the requirement of $\leq$150 ppm; however, the sample was collected in a water bottle that may have had a residual amount of water remaining.

Other Landing Gear Component Observations

Appendix 2 includes a preliminary test plan for analysis of the landing gear components which also includes the general visual observations of the landing gear components apart from the fracture analysis described herein. It includes also chronology of the investigation. Results of dimensional inspections are presented in Appendix 3.

CONCLUSIONS:

1) The lower and upper torque arms fractured due to ductile separation. The fractured end of the lower arm appeared to be bent slightly in an inboard direction. The fractured end of the upper arm lug was twisted in an inboard direction. The associated apex bolt was slightly bent.
2) Witness marks on the MLG cylinder and side brace links indicated that the side brace assembly had become hyper-extended and crossed over the cylinder during the incident. Fracture #1 through the upper side brace link occurred due to ductile separation. The fracture through the lower link exhibited evidence of intergranular separation to a crack depth of 0.05 inch. Witness/damage marks suggested that the lower link was still intact during hyper-extension of the side brace.
3) The retract cylinder rod fractured due to ductile separation. The rod was bent in an outboard direction
4) The lower lock link fractured due to ductile separation. The lower link was bent in an upward and aft direction, while the associated upper link was bent in a forward direction
5) A number of threaded inserts had partially pulled out of the shimmy damper housing. The threads in the holes of the housing appeared to have been sheared, and the ends of the holes were elongated in a circumferential direction.
6) Hardness of the lower lock link was slightly higher than the specified range. No other anomalies were observed.
7) A sample of hydraulic fluid was collected from the shock strut at the incident site and results of the analysis are detailed in Appendix 1.
8) General visual observations of the overall investigation were summarized in Appendix 2 and dimensional measurements taken were documented in Appendix 3.

[redacted]

[redacted]

ACKNOWLEDGEMENTS:

[redacted] – Photography, Metallography, & Hardness
[redacted] – Scanning Electron Microscopy
[redacted] – Chemistry

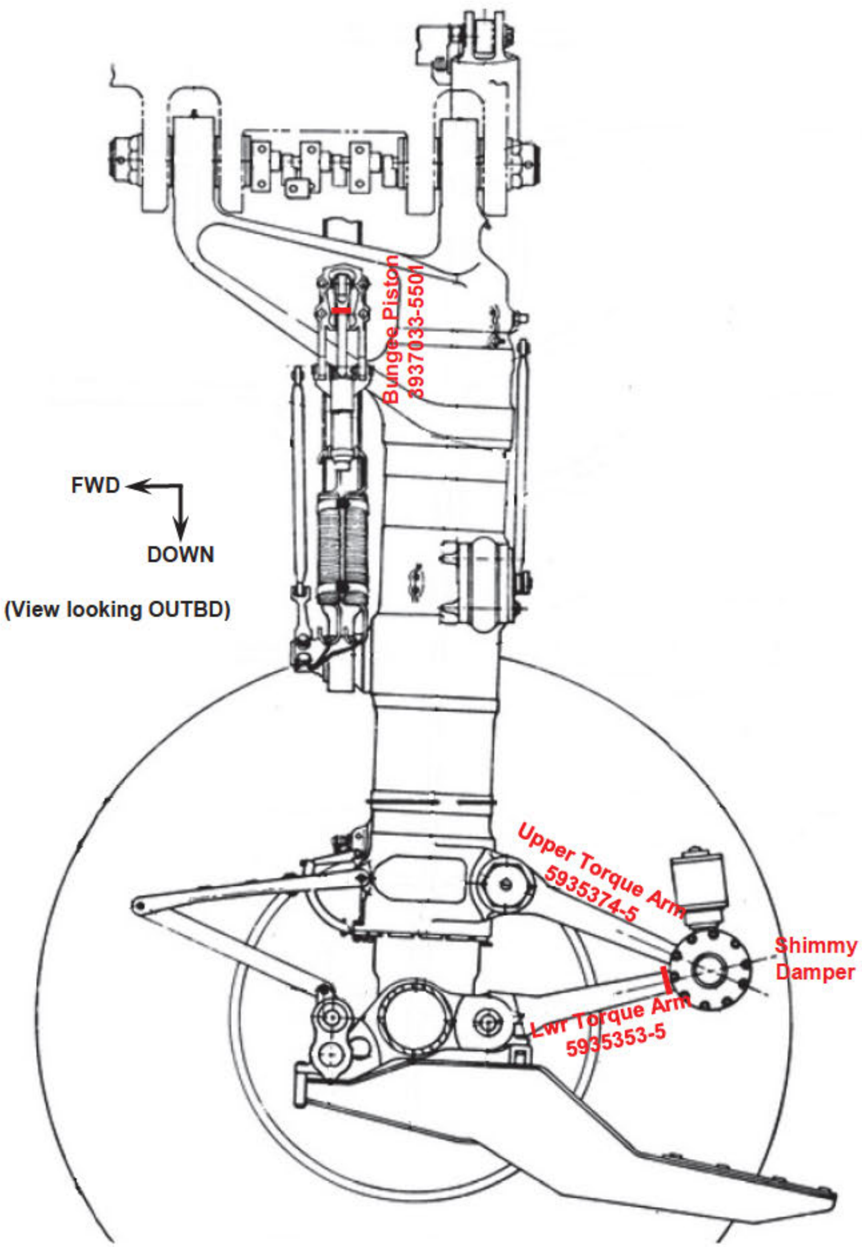

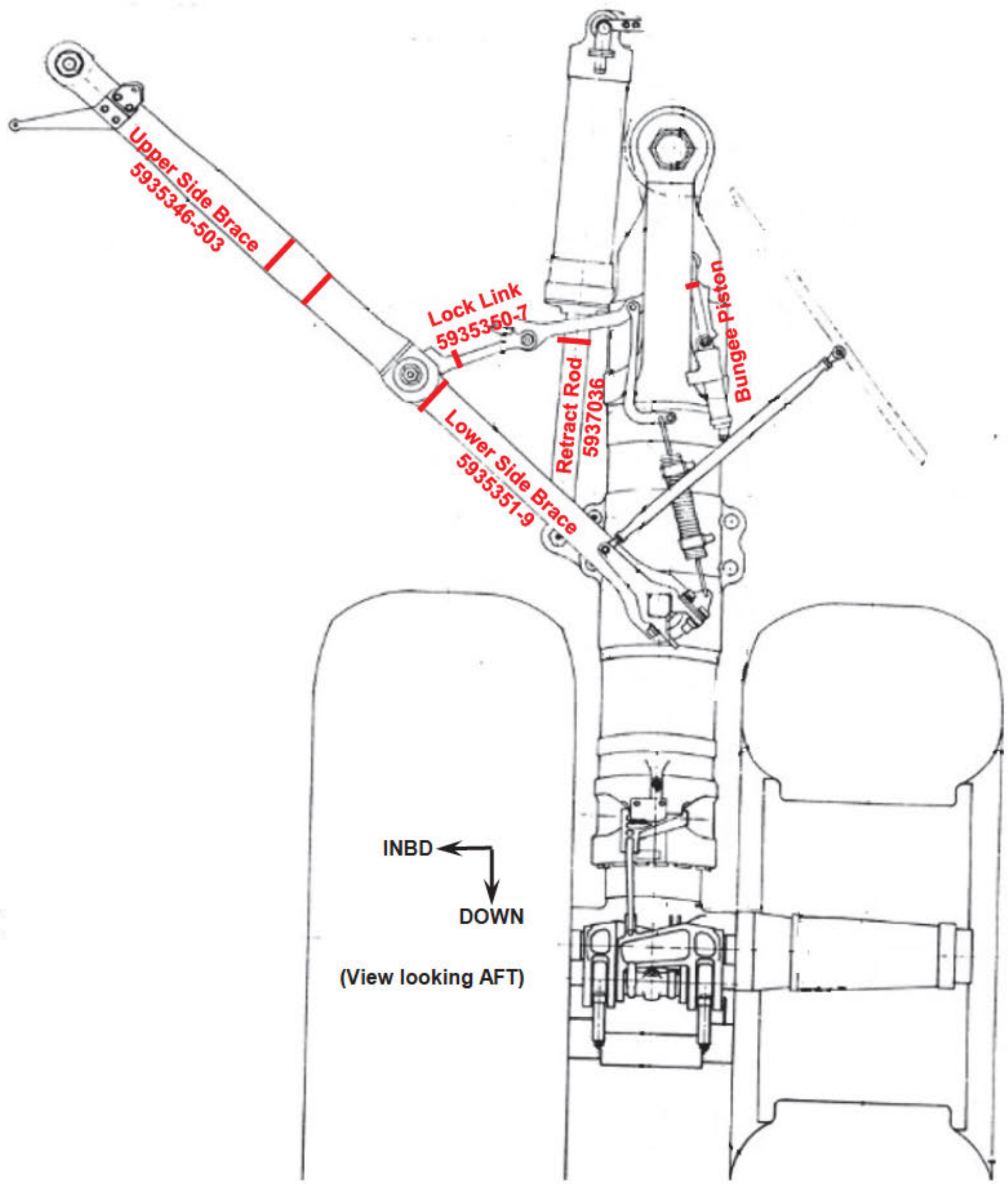

Figures 1 and 2. Illustrations showing typical MLG assembly. (Red lines indicate fracture locations.)

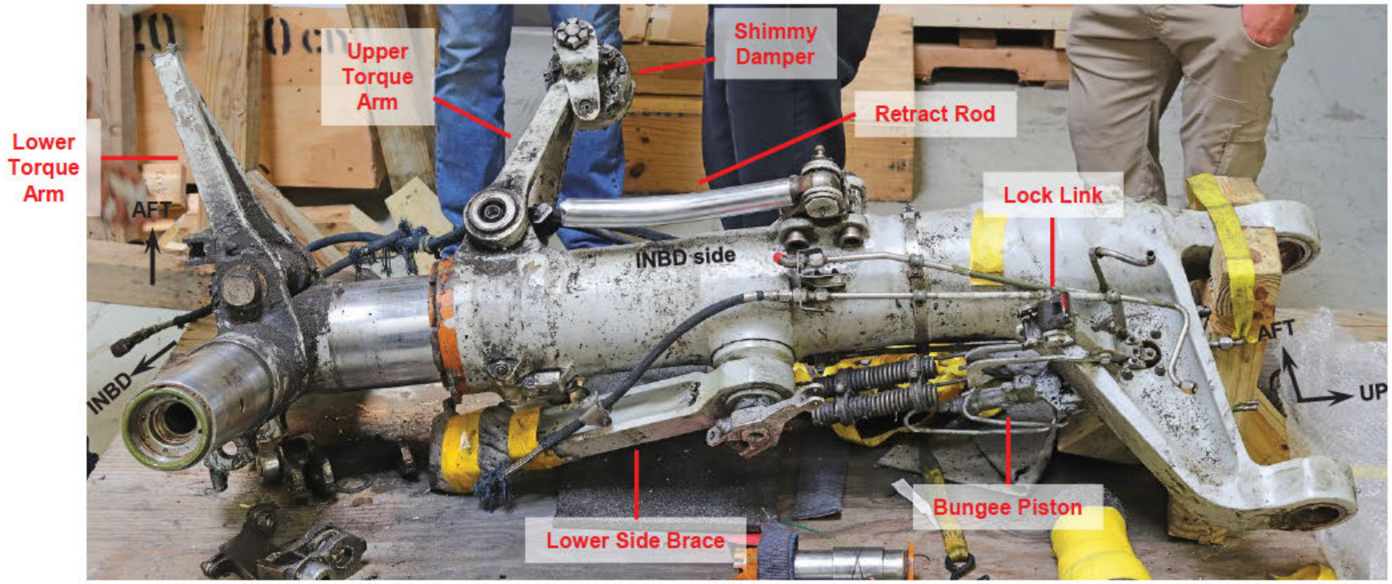

Figure 3. Overall of MLG assembly in as-received condition [axle rotated 45° clockwise relative to cylinder]

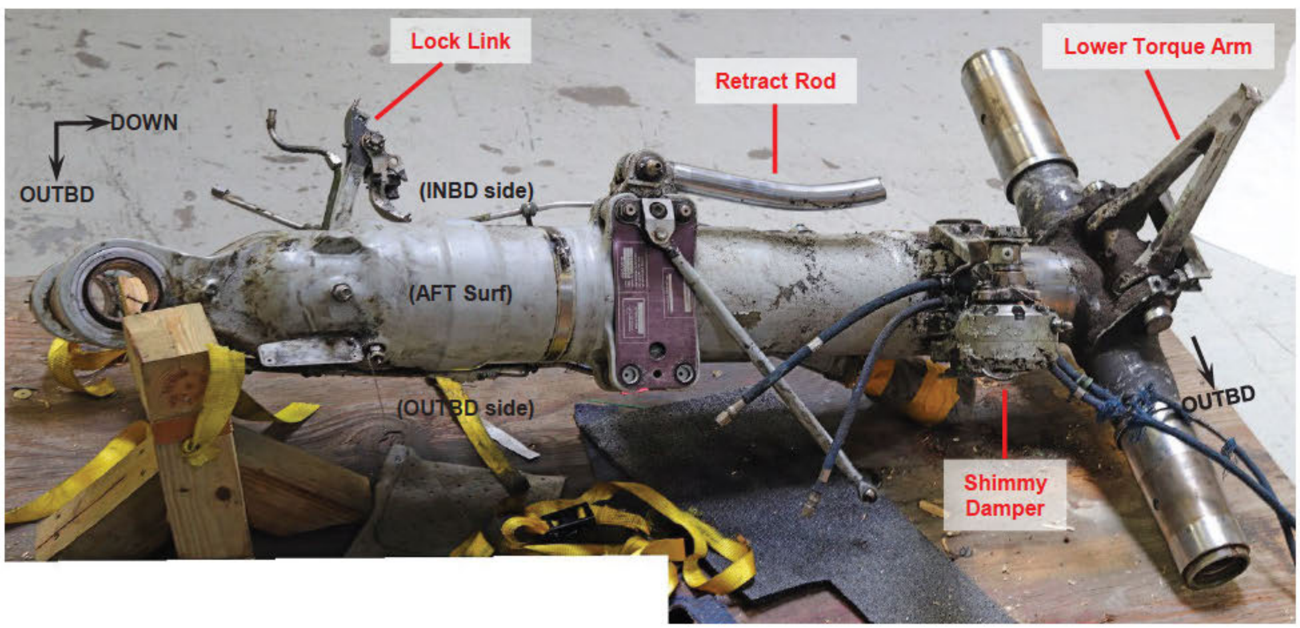

Figure 4. Overall of MLG assembly in as-received condition [cylinder and axle rotated 45° relative to each other]

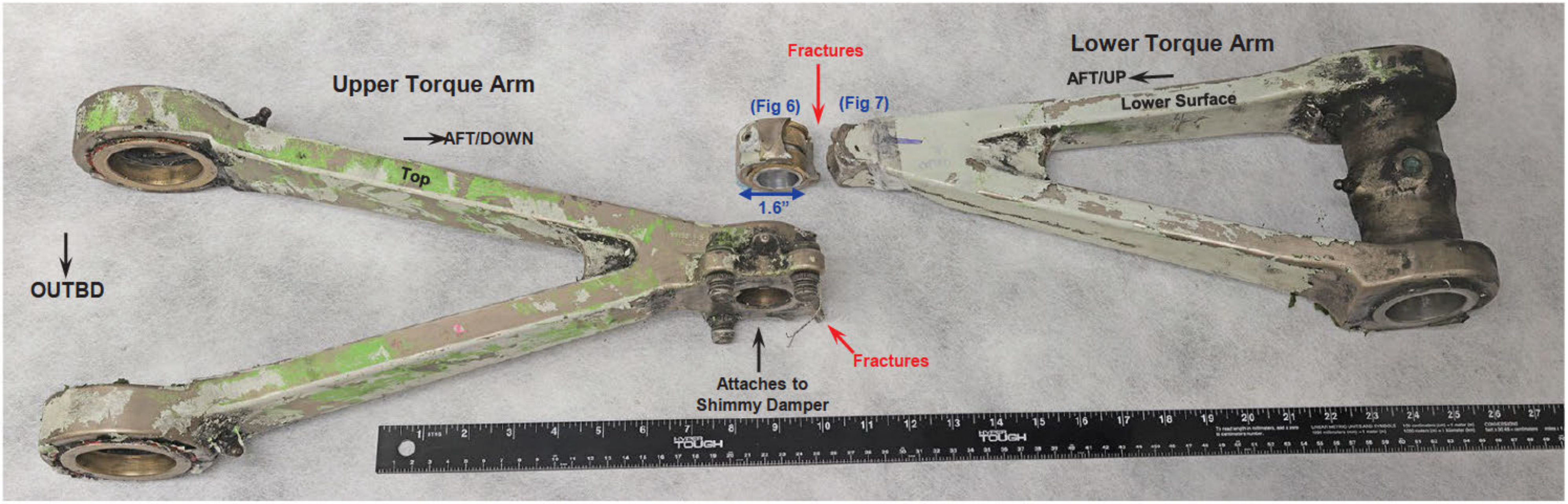

Figure 5. Overall of upper and lower Torque Arms [paint partially stripped from upper Arm in lab].

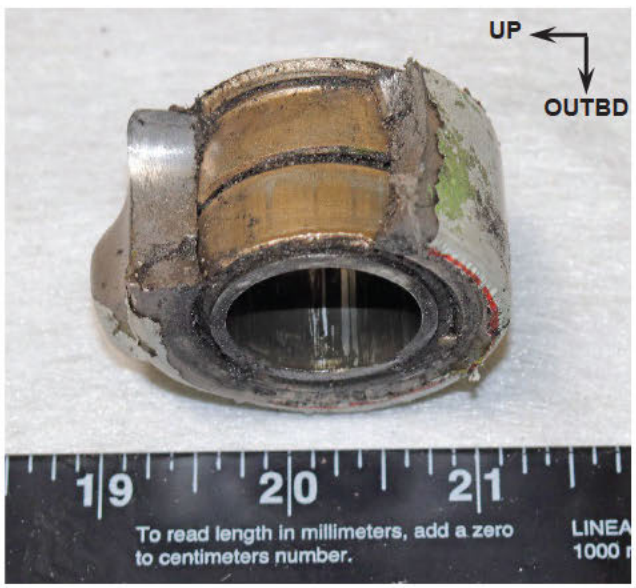

Figure 6. Close-up of fracture surfaces of Lower Torque Arm

Figure 7. Close-up of mating fracture surfaces of Lower Torque Arm

Figure 8. Overall of upper Torque Arm

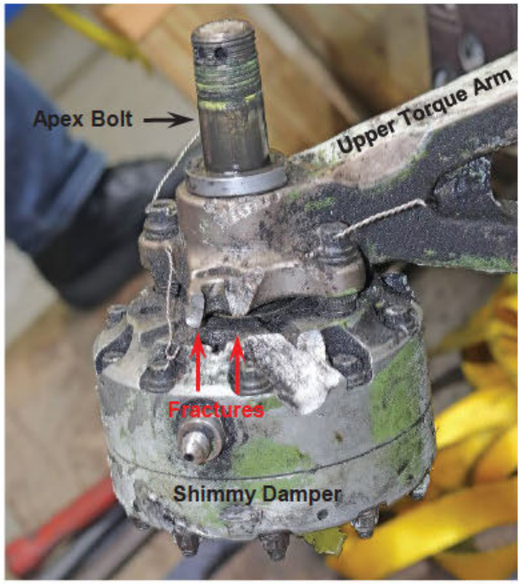

Figure 9. Close-up of fracture surfaces on Upper Torque Arm with the Shimmy Damper and Apex Bolt attached

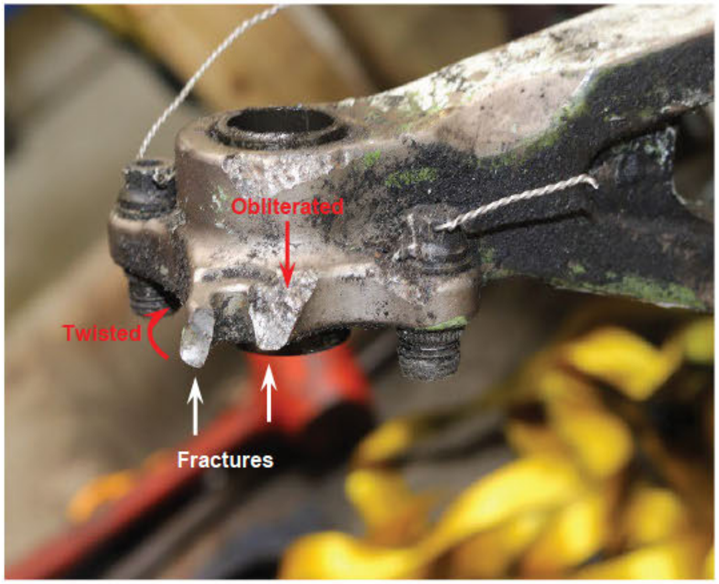

Figure 10. Close-up of mating fracture surfaces on the Upper Torque Arm

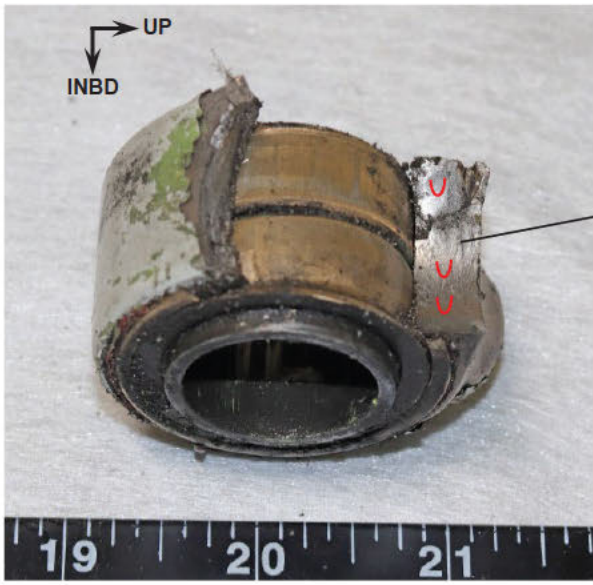

Figure 11. Close-up of fracture surfaces Red ellipses indicate direction of open-ended dimple formations. [Lower Torque Arm]

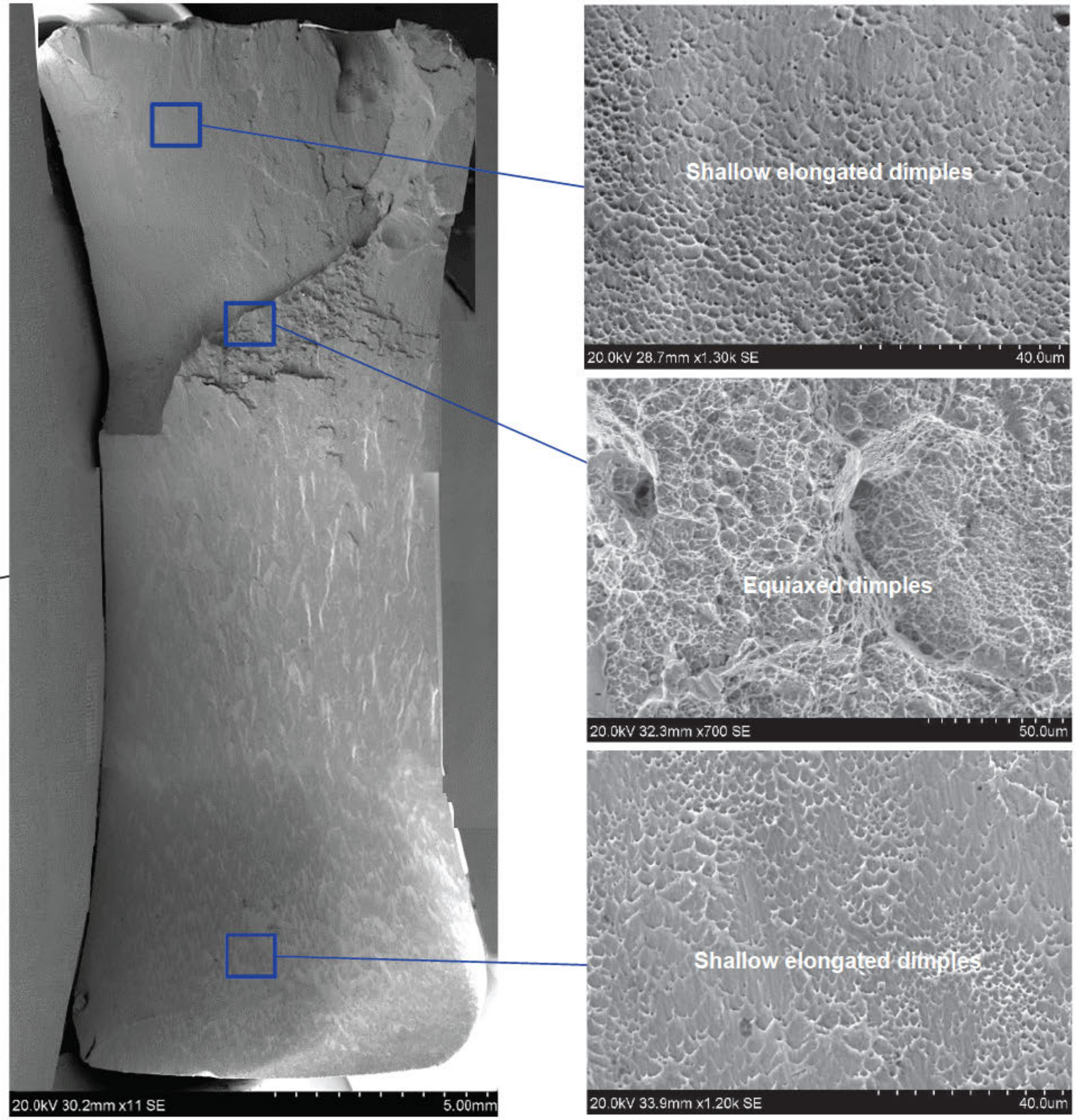

Figures 12 to 15. SEM close-ups from upper fracture segment

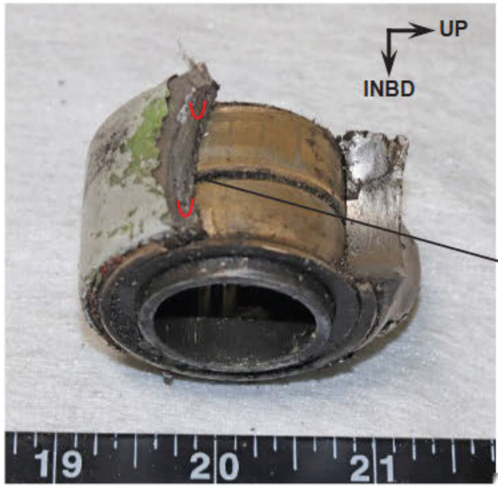

Figure 16. Close-up of fracture surfaces Red ellipses indicate direction of open-ended dimple formations. [Lower Torque Arm]

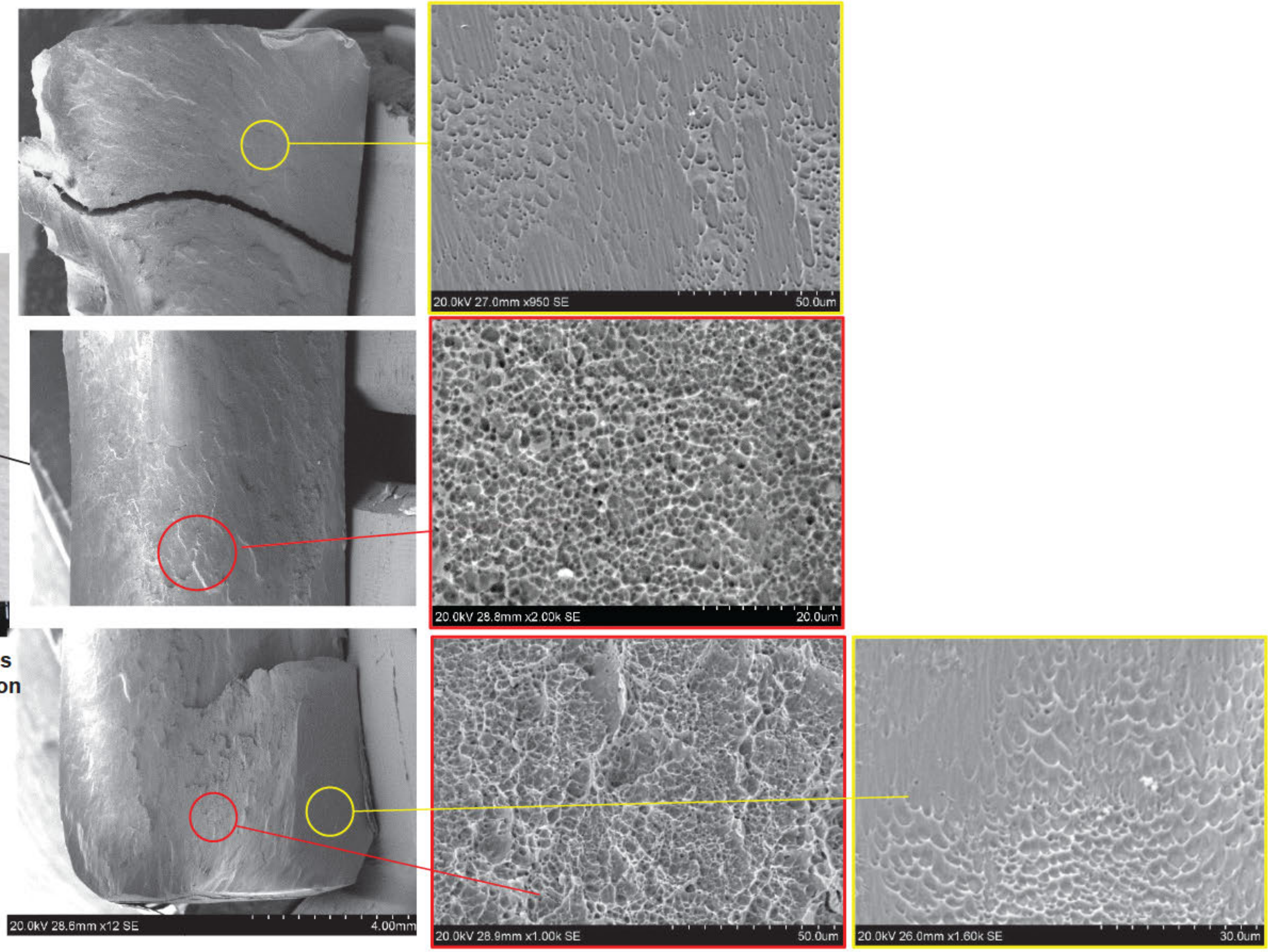

Figures 17 to 23. SEM close-ups from lower fracture segment

Figure 24. Close-up of mating fracture surface [Lower Torque Arm]

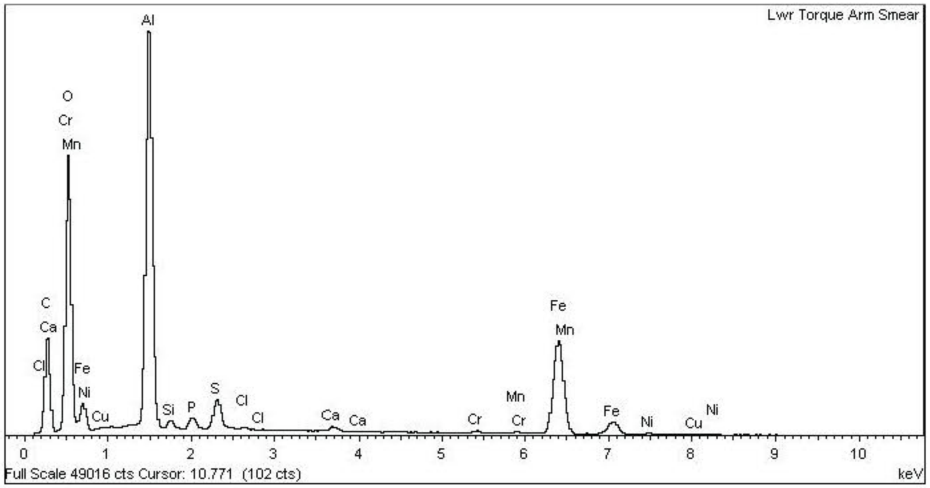

Figure 25. EDS spectrum from smeared metal on fracture surface

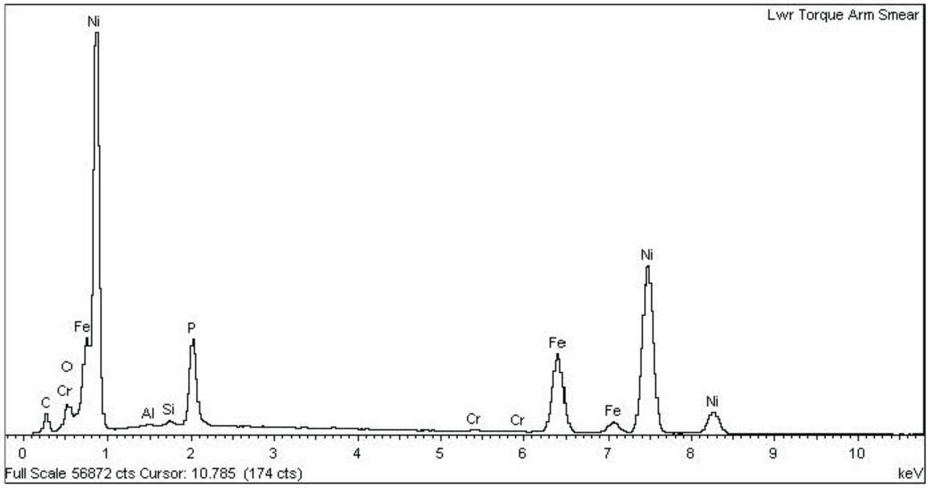

Figure 26. EDS spectrum from smeared metal on fracture surface

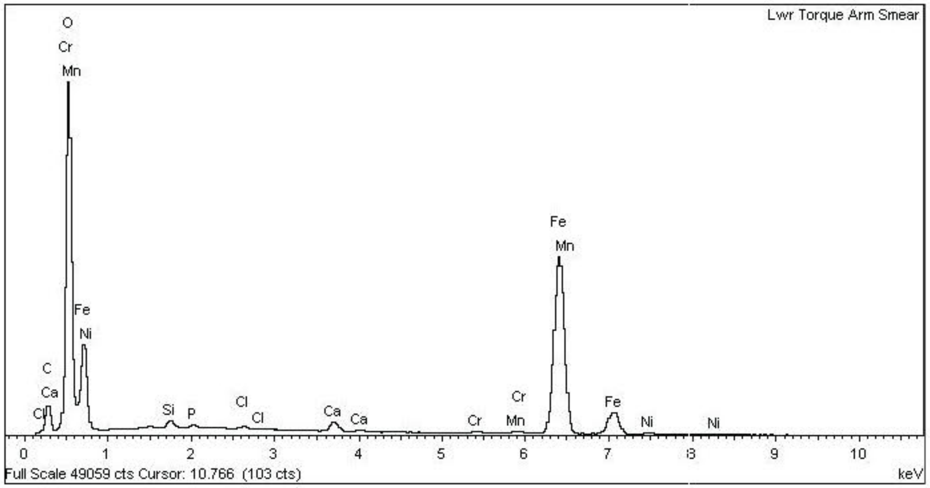

Figure 27. EDS spectrum from rust on fracture surface

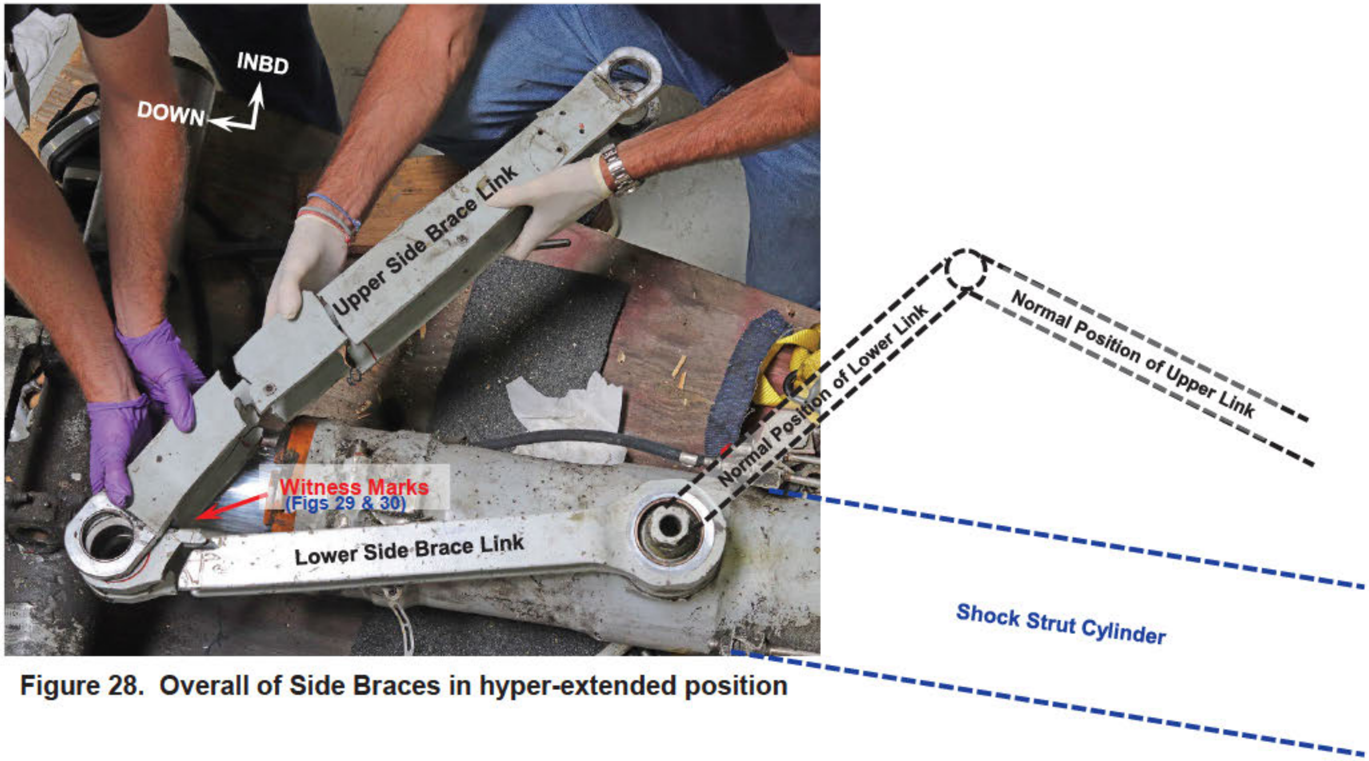

Figure 28. Overall of Side Braces in hyper-extended position

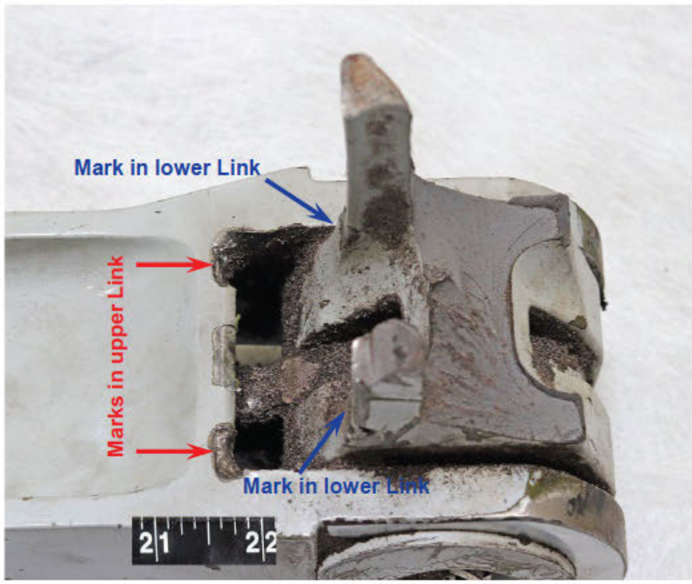

Figures 29 and 30. Close-up of witness marks in Links from contact during hyper-extension

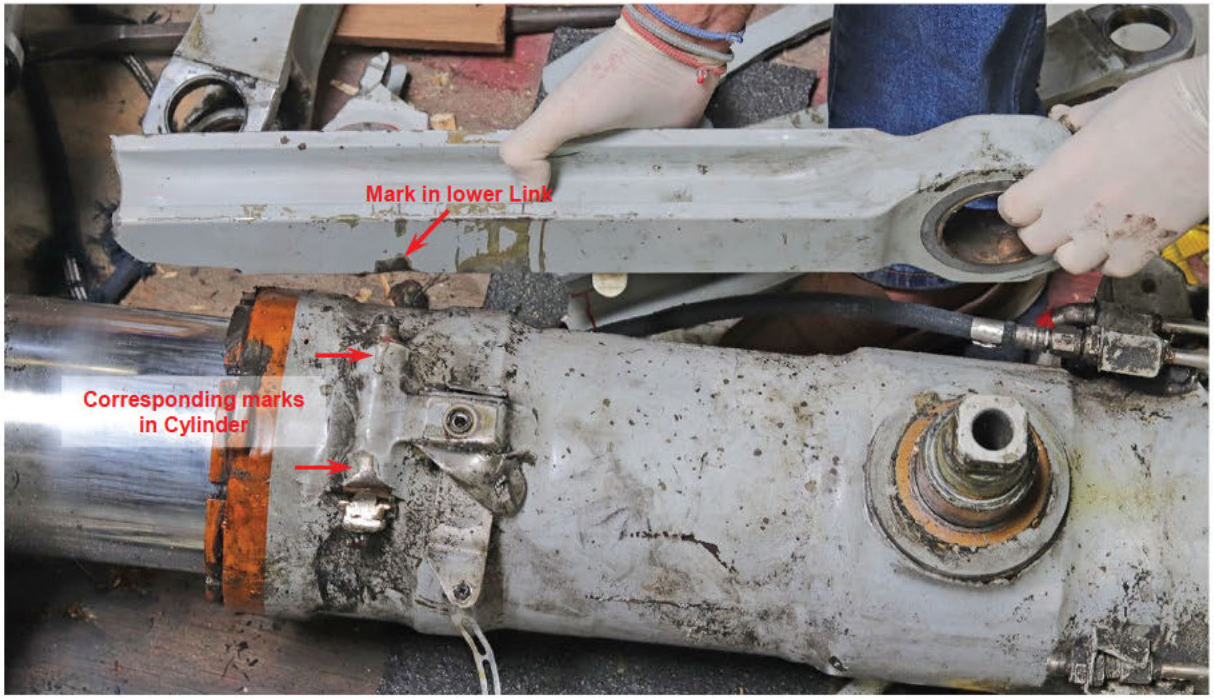

Figures 31. Close-up of witness marks in Cylinder from contact with Links during hyper-extension

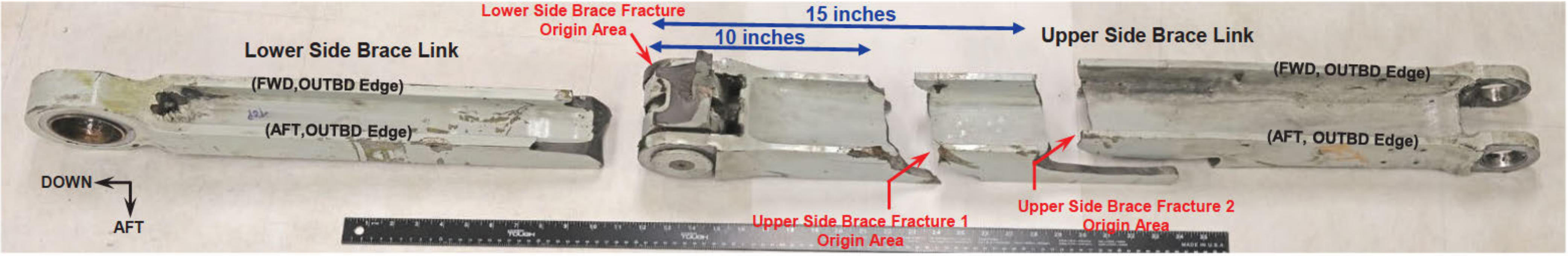

Figure 32. Overall of Side Brace Links in extended position

Upper Side Brace Link

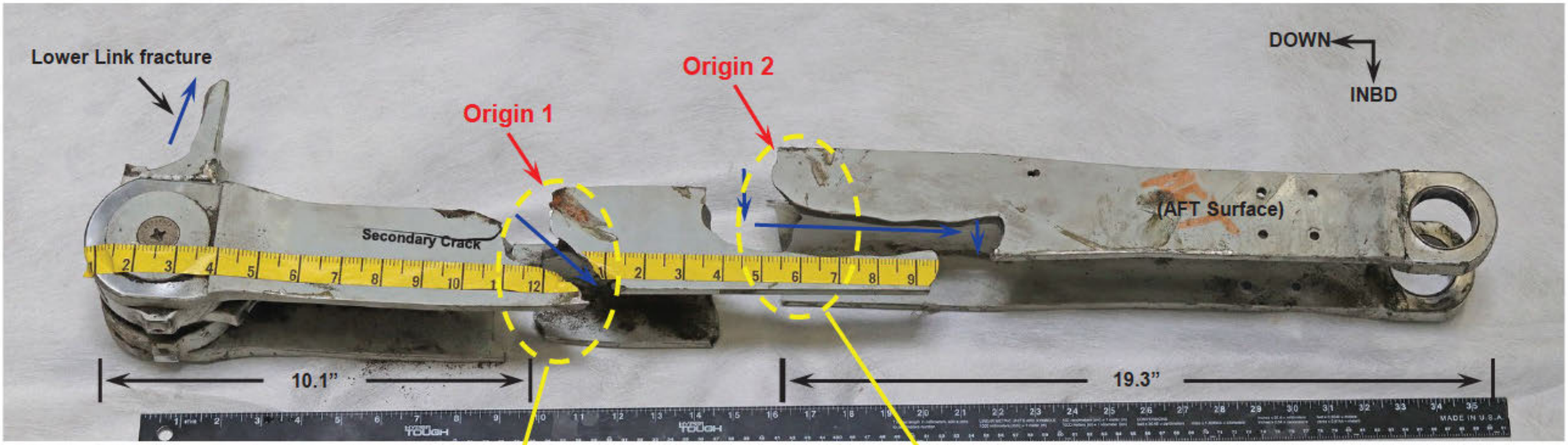

Figure 33. Overall of upper Side Brace Link [Blue arrows indicate directions of crack propagation]

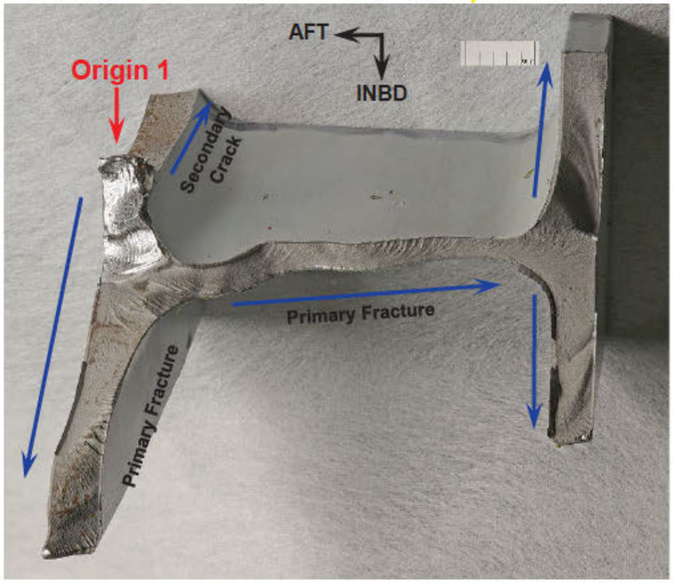

Figure 34. Close-up of Fracture 1
[Blue arrows indicate directions of crack propagation]

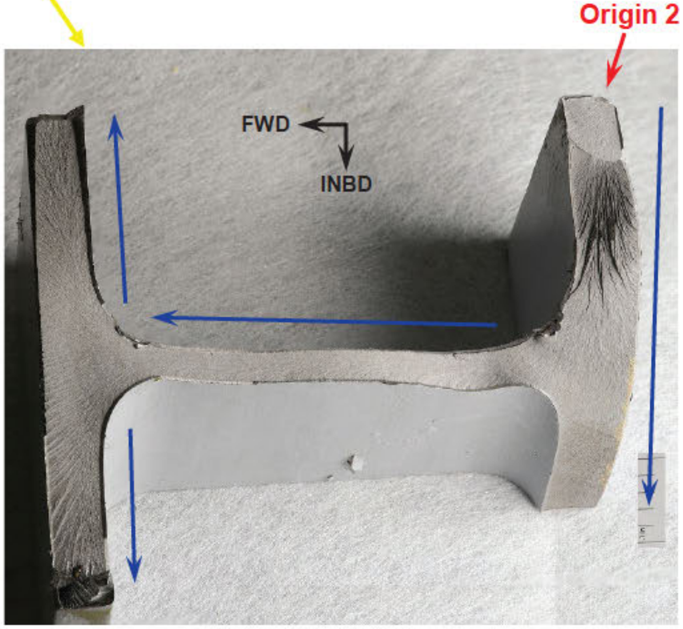

Figure 35. Close-up of Fracture 2
[Blue arrows indicate directions of crack propagation]

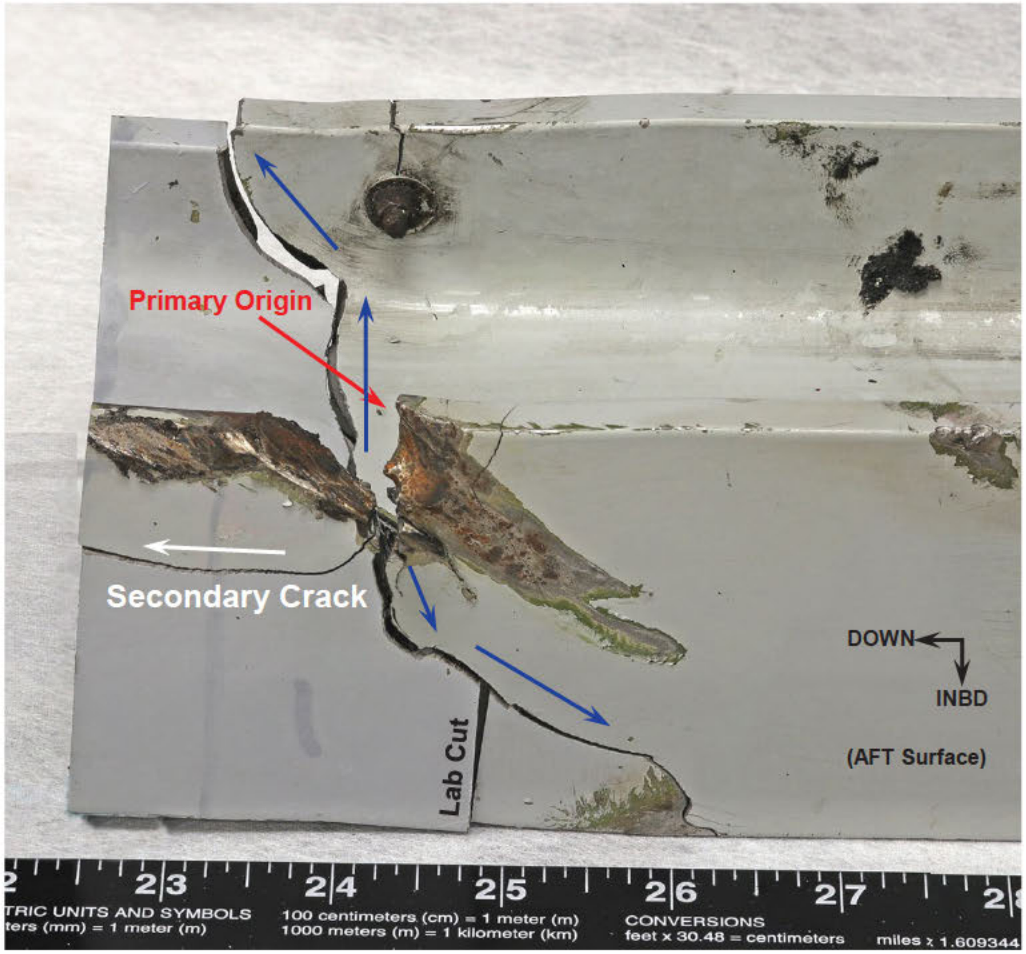

Figure 36. Close-up of Fracture 1 and adjacent secondary crack in Upper Side Brace Link
[Blue arrows indicate directions of primary crack propagation]
[White arrow indicates direction of secondary crack propagation]

Figure 37. Close-up of secondary origin area.

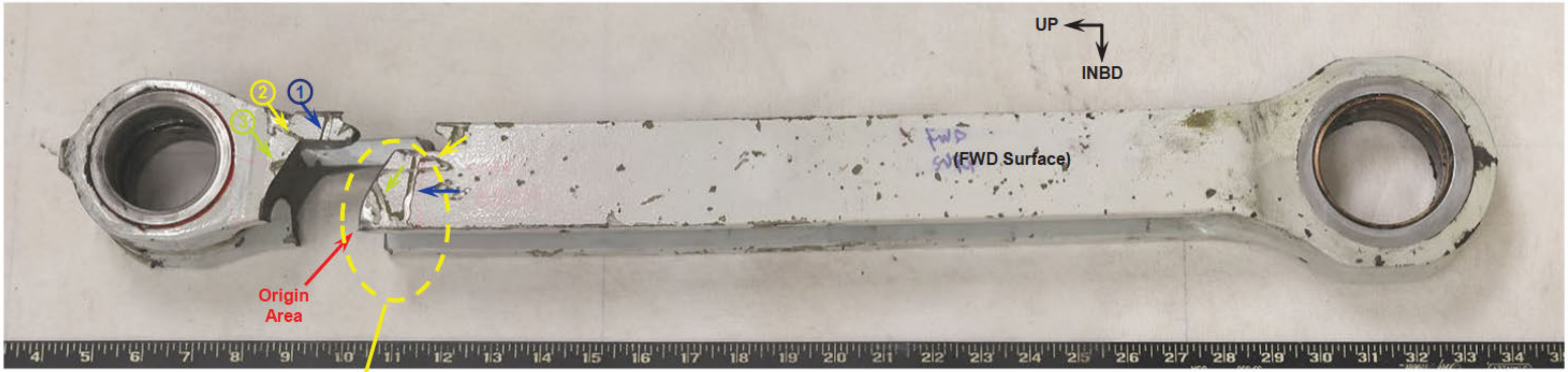

Figure 38. Overall of Lower Side Brace [Blue, yellow, and green arrows indicate areas of matching witness marks].

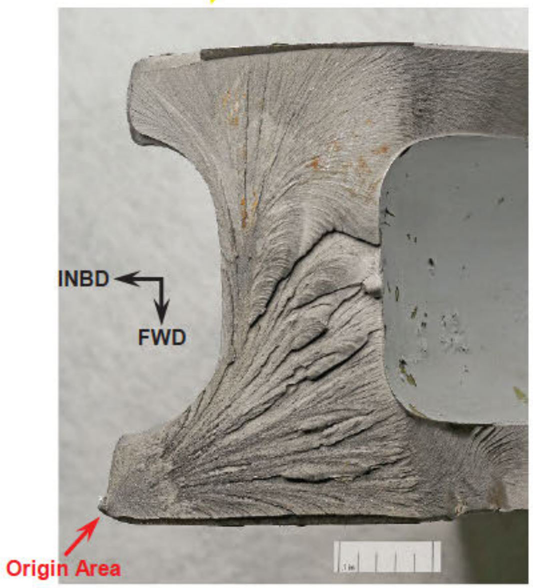

Figure 39. Close-up of fracture surface

Figure 40. Close-up of origin area

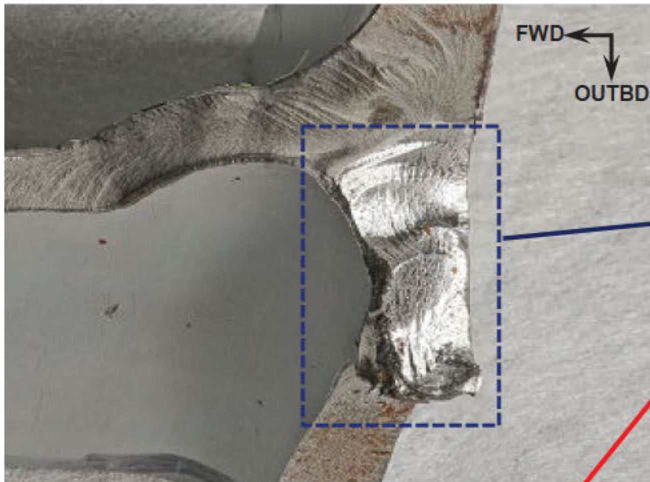

Figure 41. Close-up of origin area [Upper Side Brace Fracture 1]

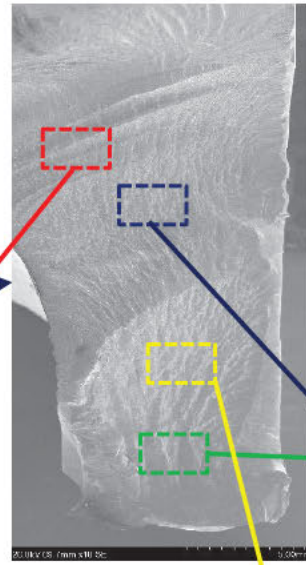

Figure 42. SEM close-up of origin area

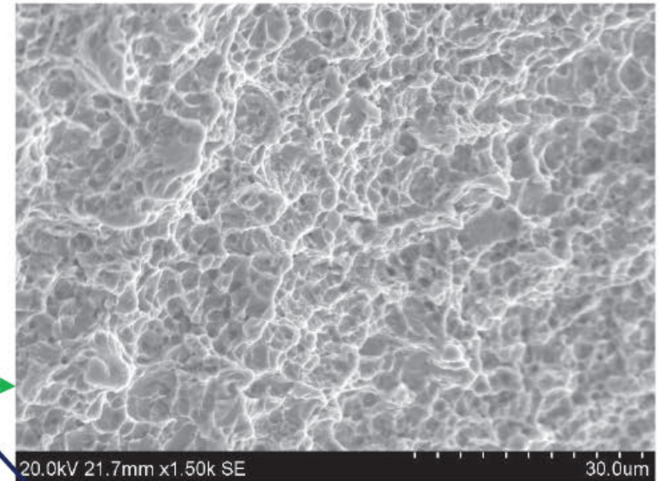

Figure 43. SEM close-up of origin area

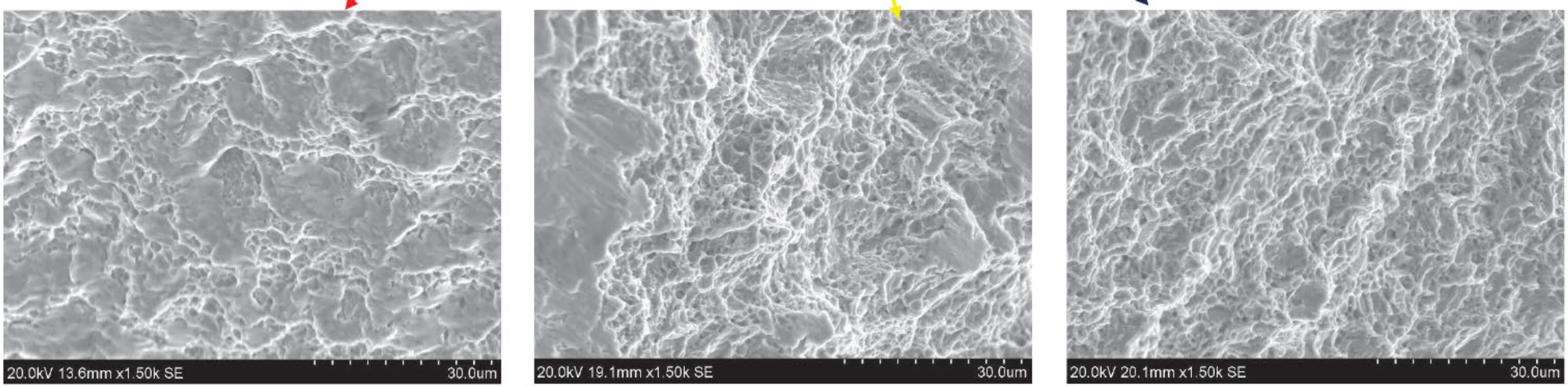

Figures 44 to 46. SEM close-ups from origin area [Upper Side Brace]

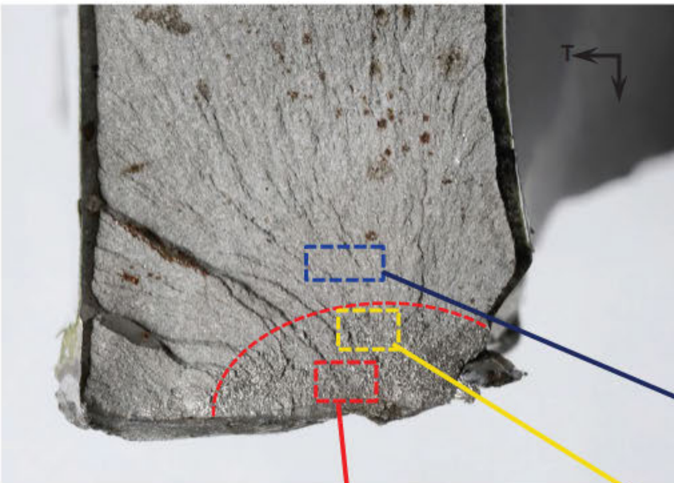

Figure 47. Close-up of origin area [Upper Side Brace]

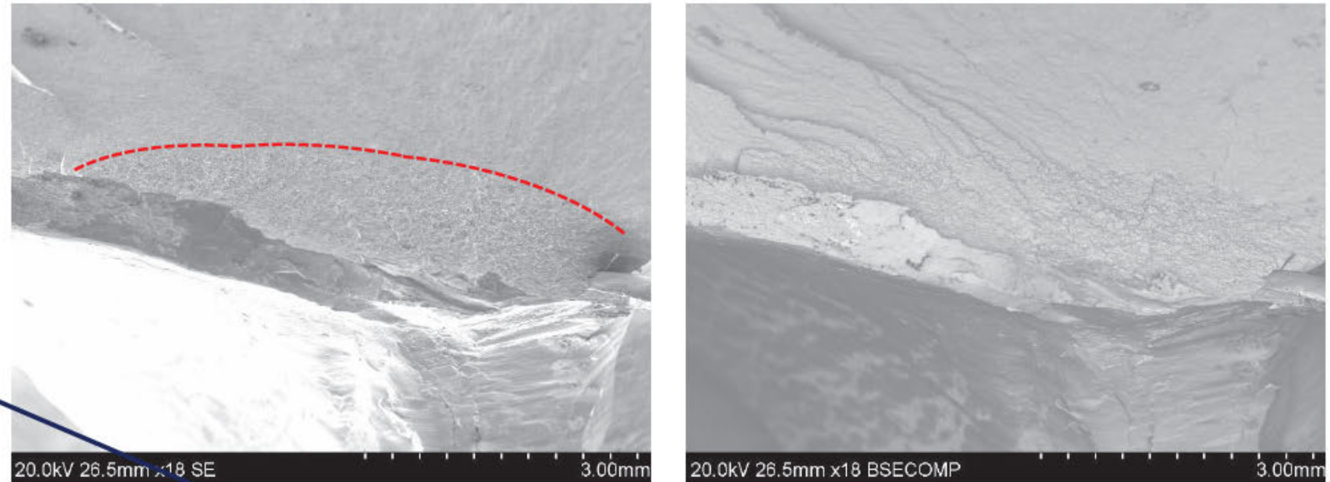

Figures 48 and 49. SEM close-ups of origin area [Upper Side Brace]

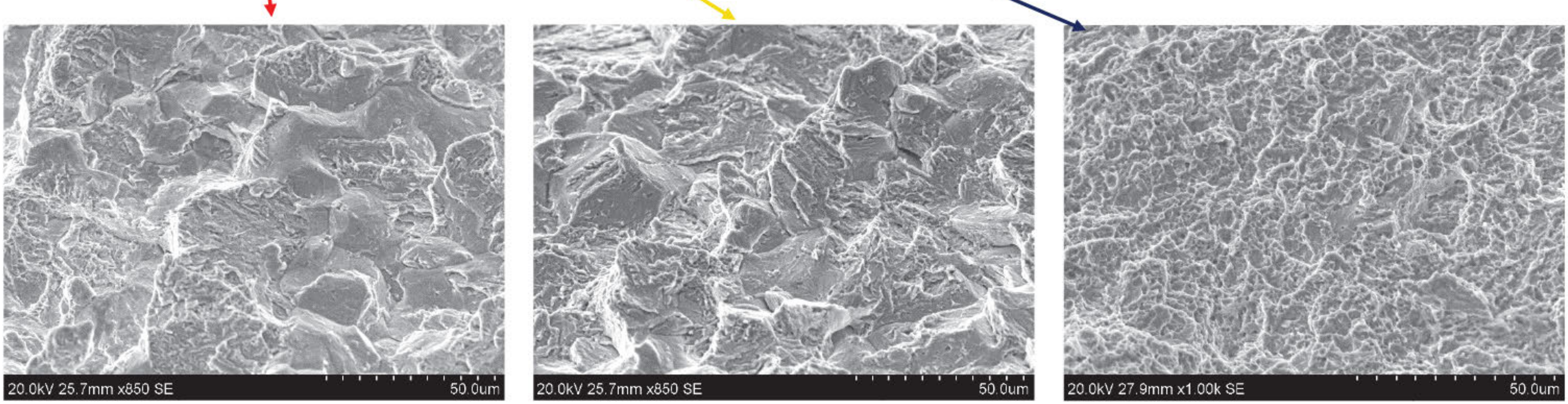

Figures 50 to 52. SEM close-ups of origin area [Upper Side Brace]

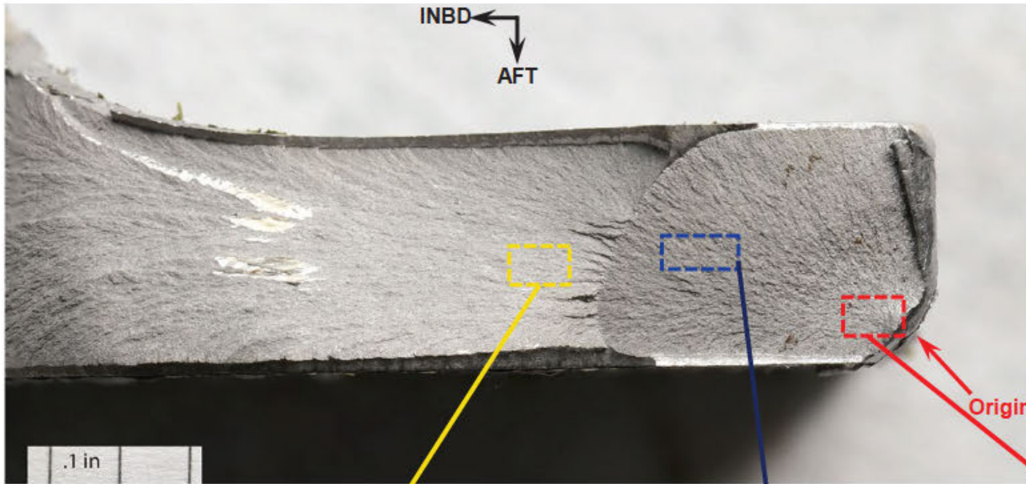

Figure 53. Close-up of origin area [Upper Side Brace Fracture 2]

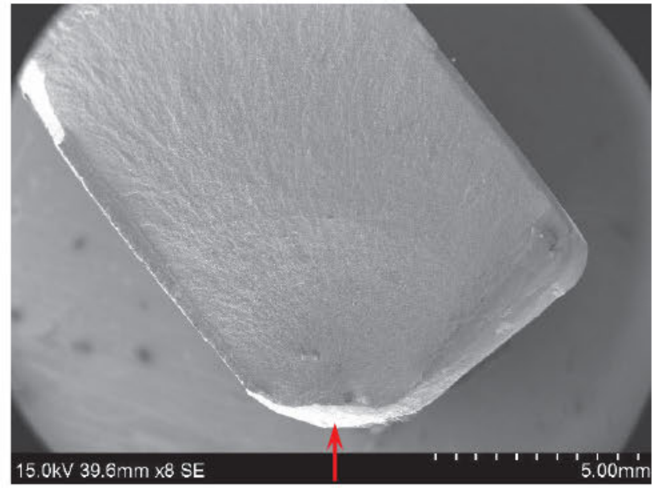

Figure 54. SEM close-up of origin area

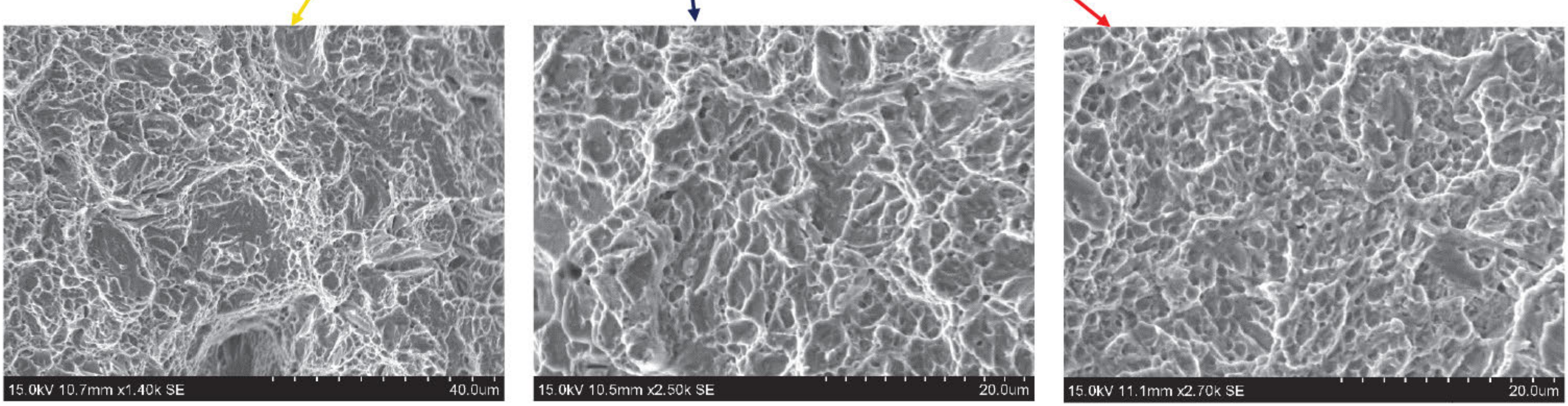

Figures 55 to 57. SEM close-ups of origin area [Upper Side Brace]

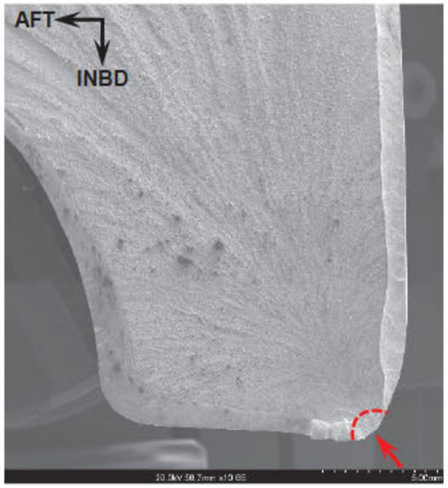

Figure 58. Close-up of origin area [Lower Side Brace]

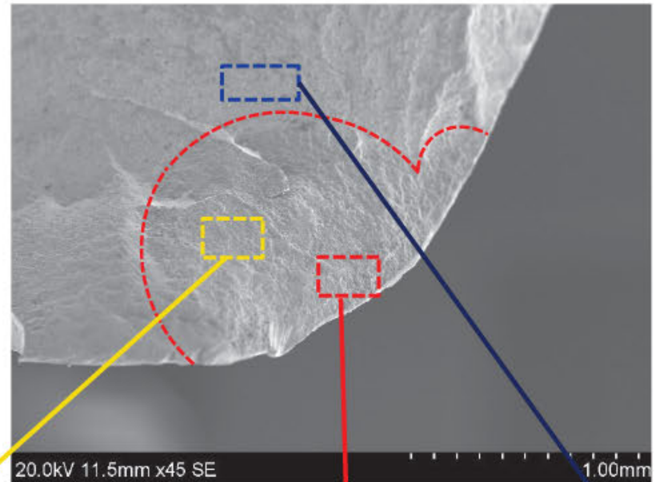

Figure 59. Close-up of origin area [Upper Side Brace Fracture 2]

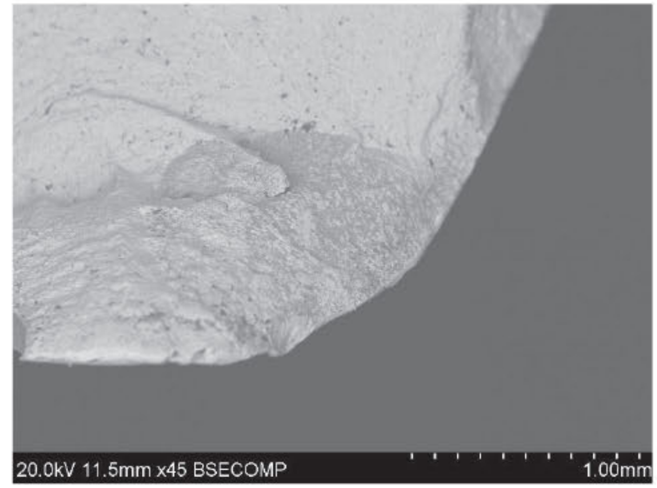

Figure 60. SEM backscatter image of origin area

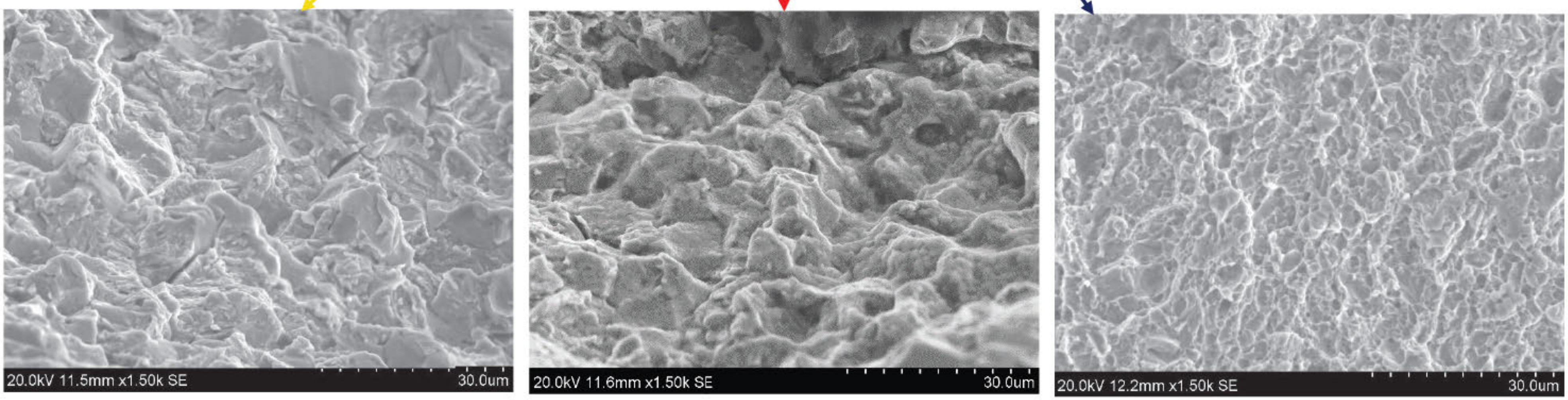

Figures 61 to 63. SEM close-ups of origin area [Low Side Brace]

Figure 64. Overall of Retract Rod [looking OUTBD]

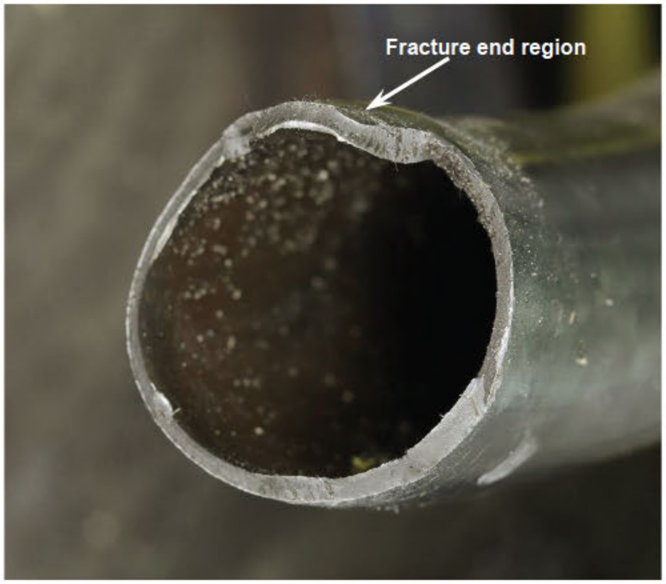

Figure 65. Close-up of fracture surface [Retract Rod]

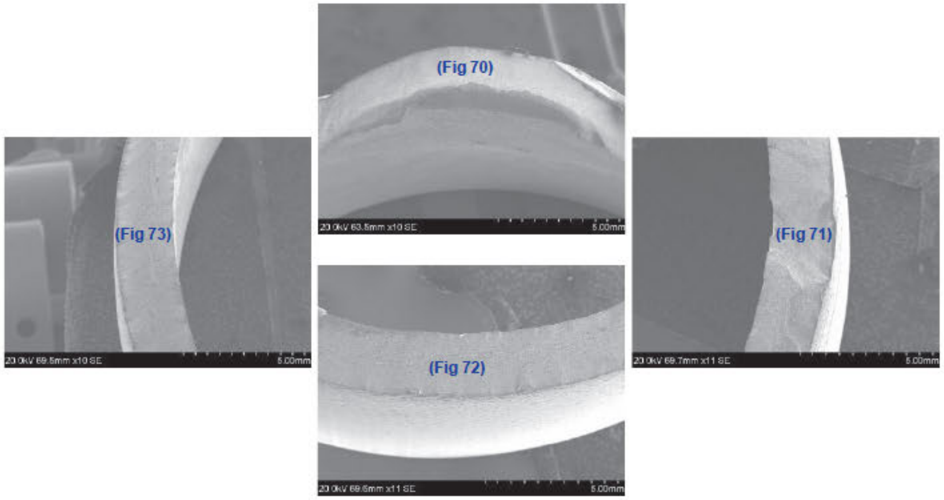

Figures 66 to 69. SEM close-ups of fracture surface [Retract Rod]

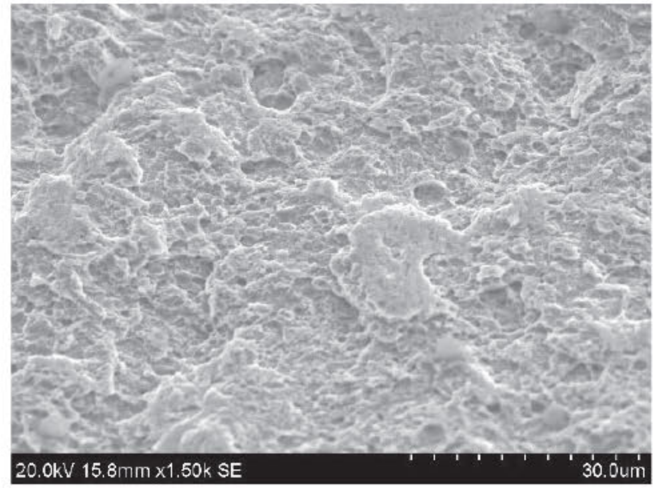

Figure 70. SEM close-up of fracture surface [Retract Rod]

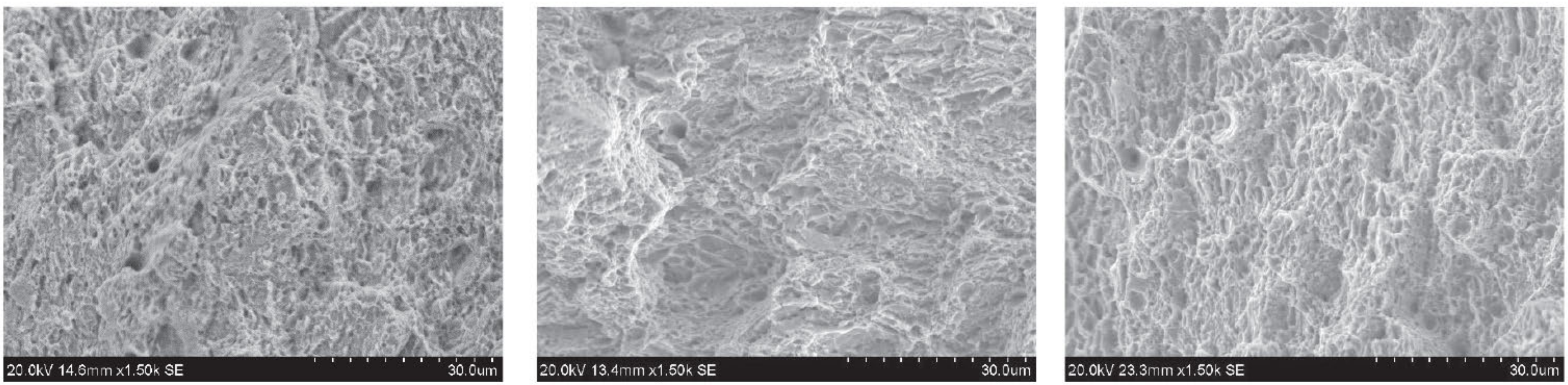

Figures 71 to 73. SEM close-ups of fracture surface [Retract Rod]

Figure 74. Close-up of Lock Links

Figure 75. Close-up of Lock Links

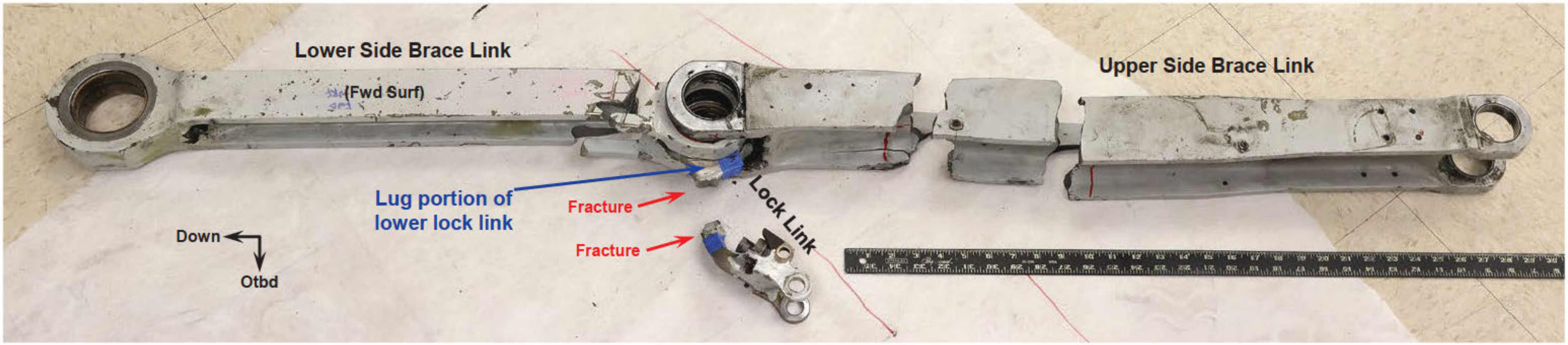

Figure 76. Close-up of Side Braces with Lock Link intact

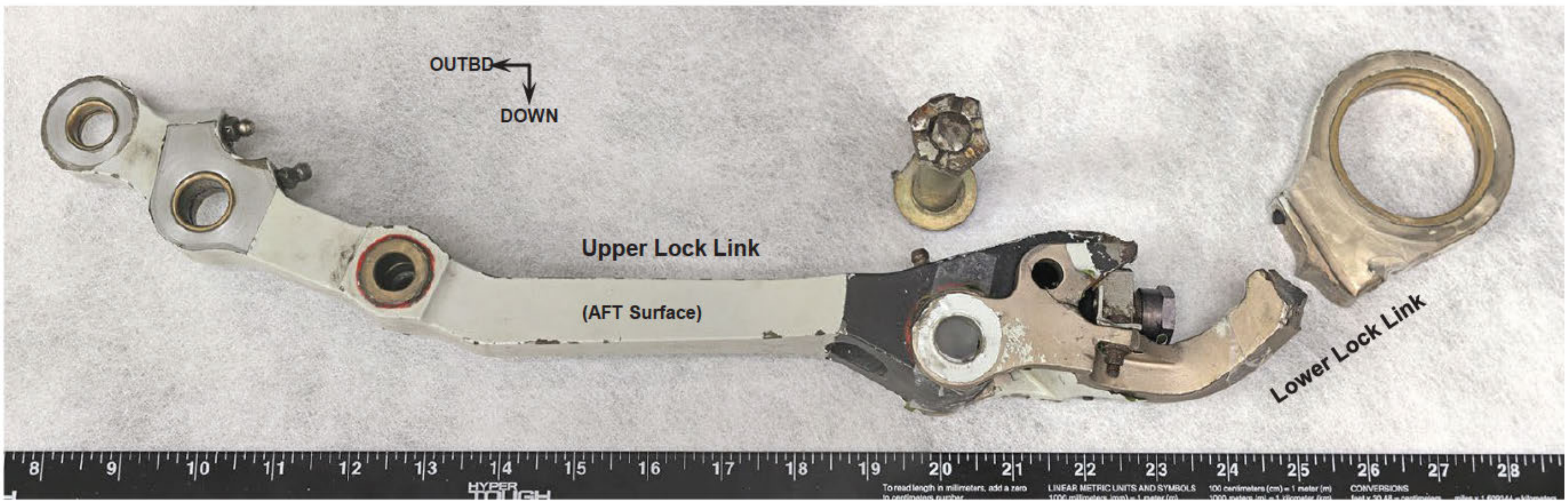

Figures 77 and 78. Close-ups of Lock Links after removal

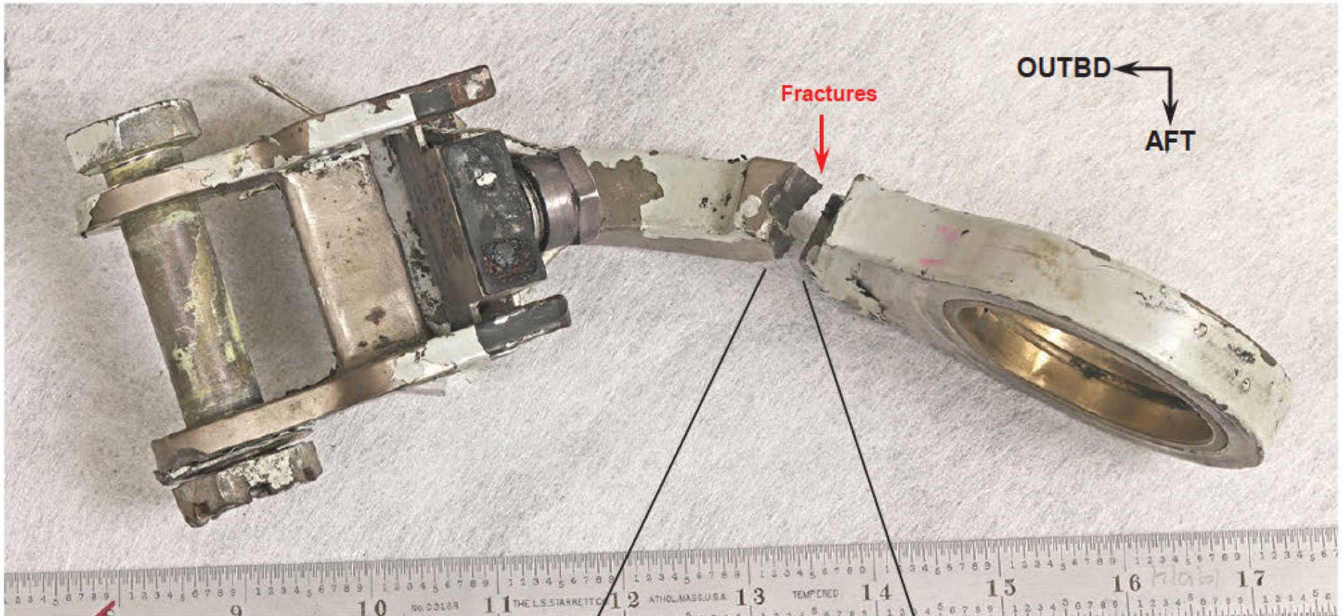

Figure 79. Close-up of lower Lock Link after removal

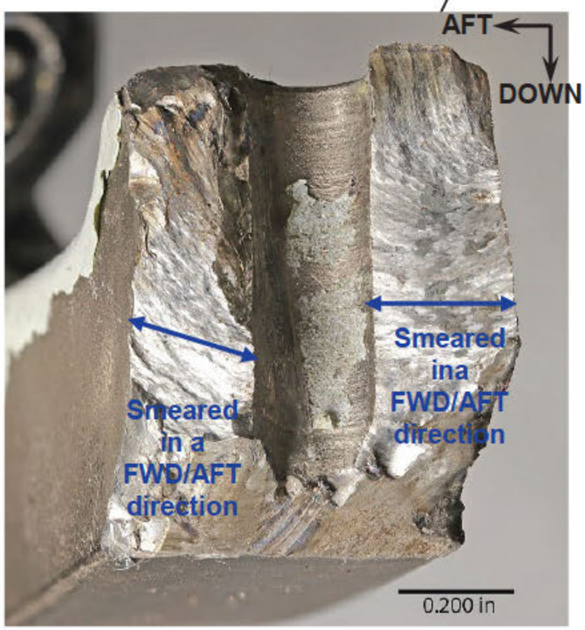

Figures 80 and 81. Close-ups of fracture surfaces [Lower Lock Link]

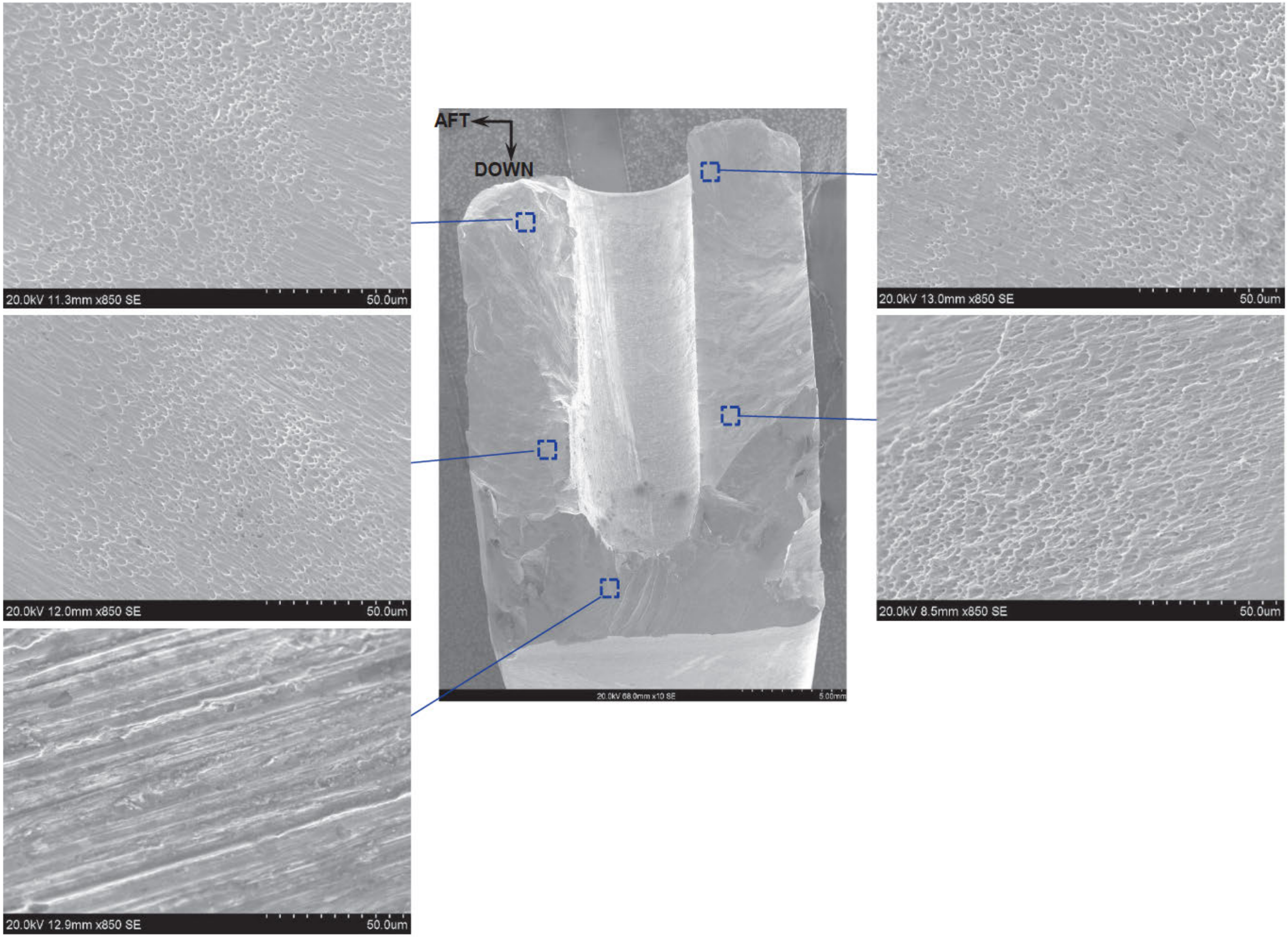

Figures 82 to 87. SEM close-ups from fracture surfaces [Lock Link]

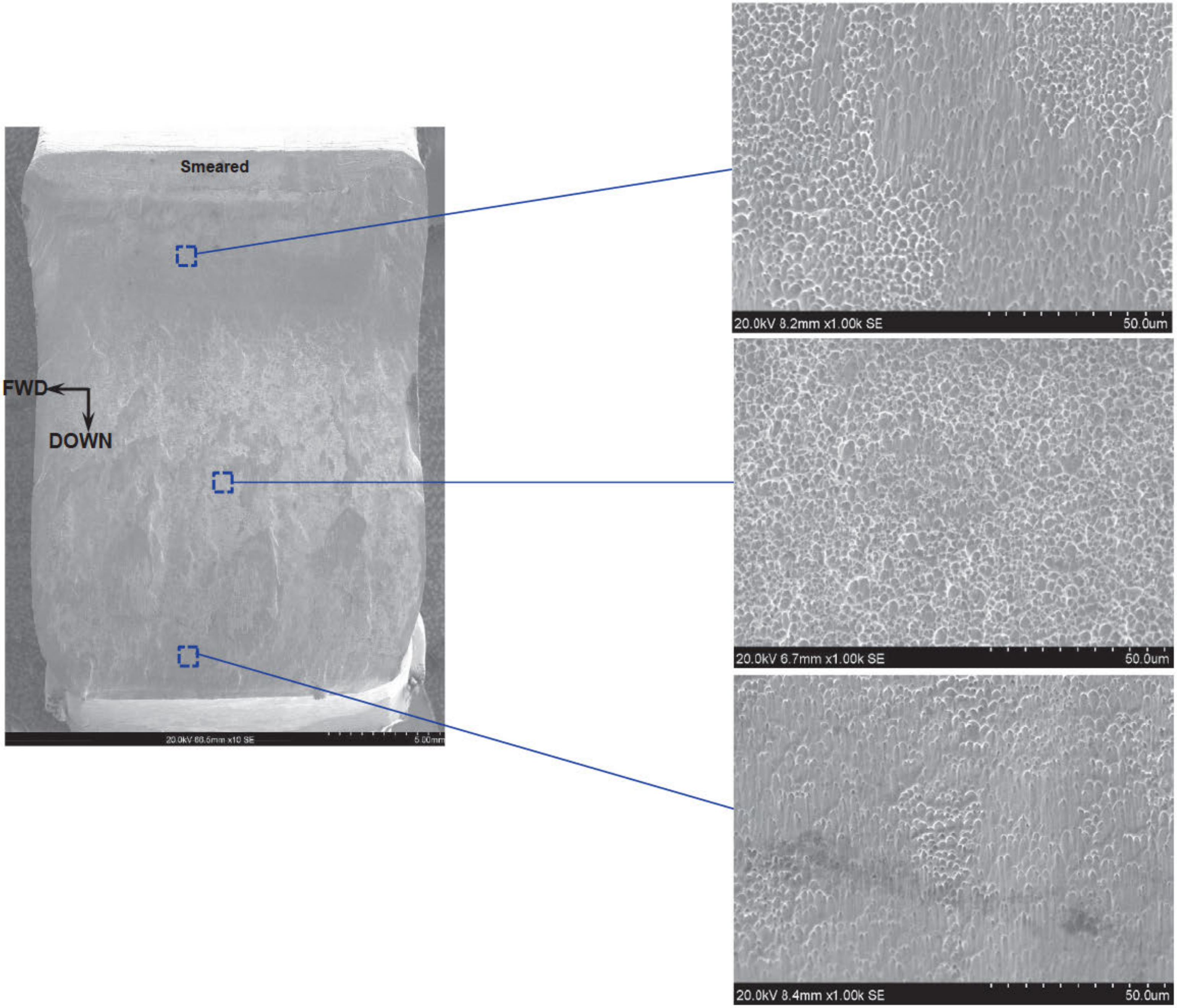

Figures 88 to 91. SEM close-ups from second fracture [Lock Link]

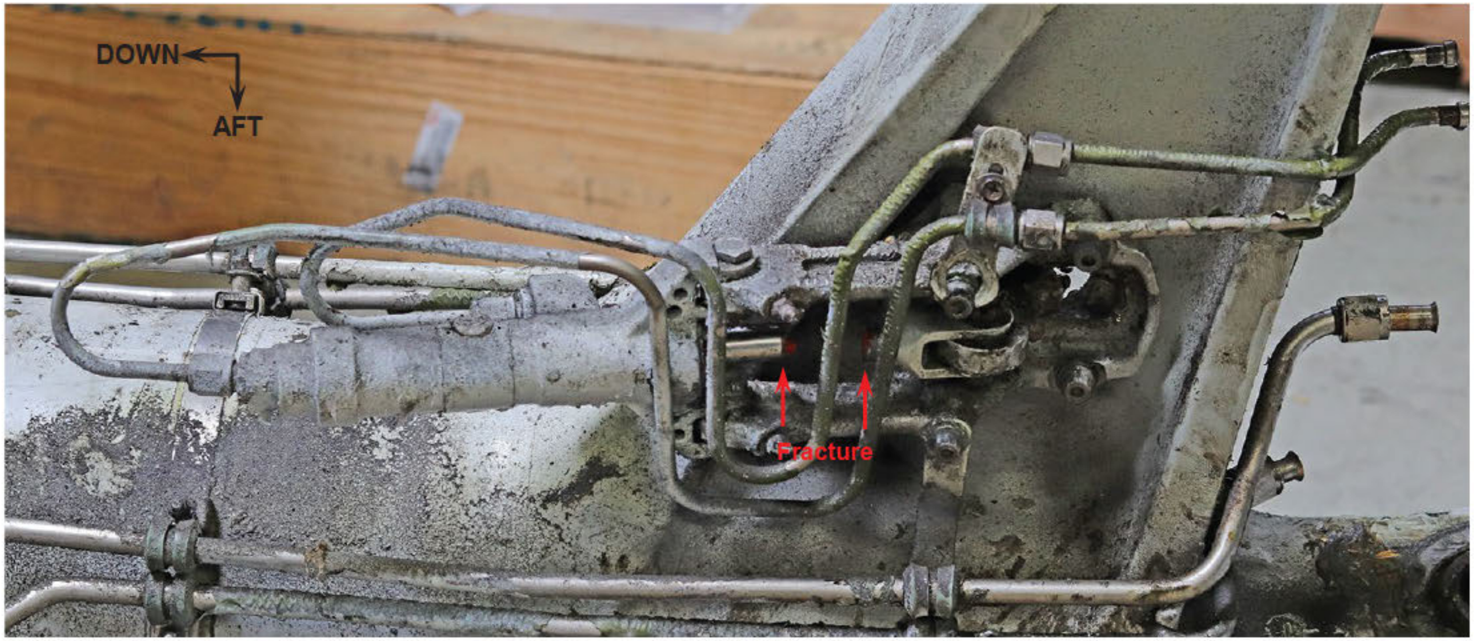

Figure 92. Close-up of fractured Bungee Piston [looking Inbd]

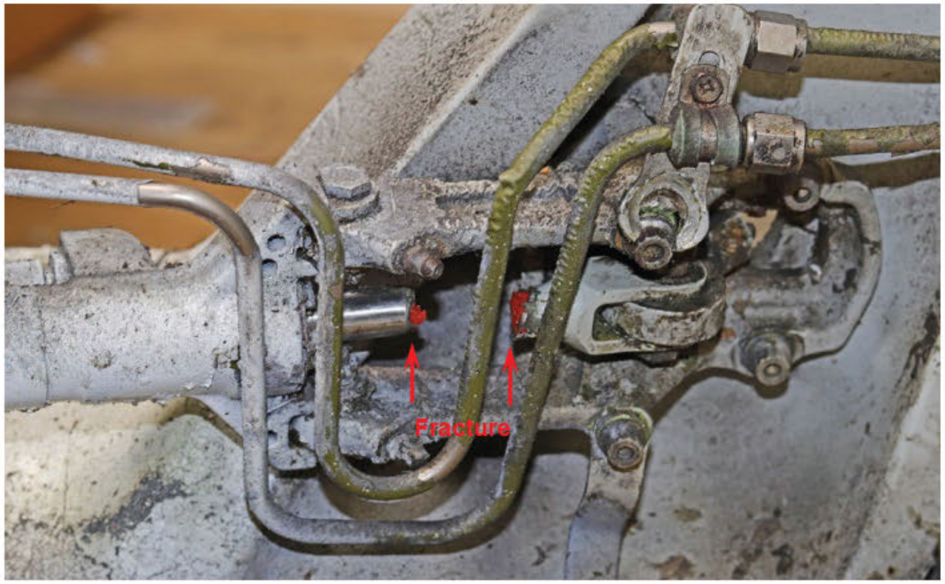

Figure 93. Close-up of fractured Bungee Piston

Figure 94. Close-up of fractured Bungee Piston after removal

Figure 95. Close-up of fracture surface at cylinder end

Figure 96. Close-up of fracture surface at clevis lug end

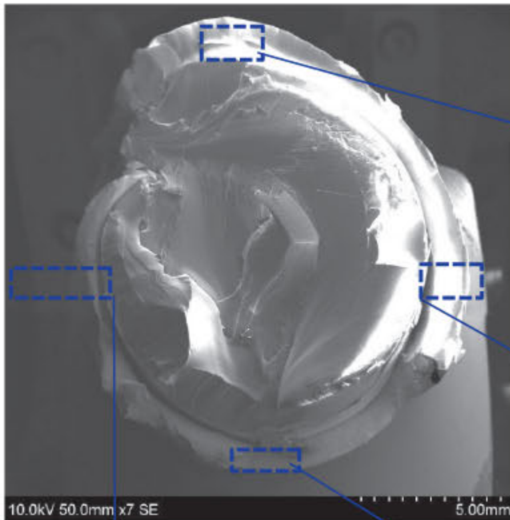

Figure 97. SEM close-up of fracture surface [Bungee Piston]

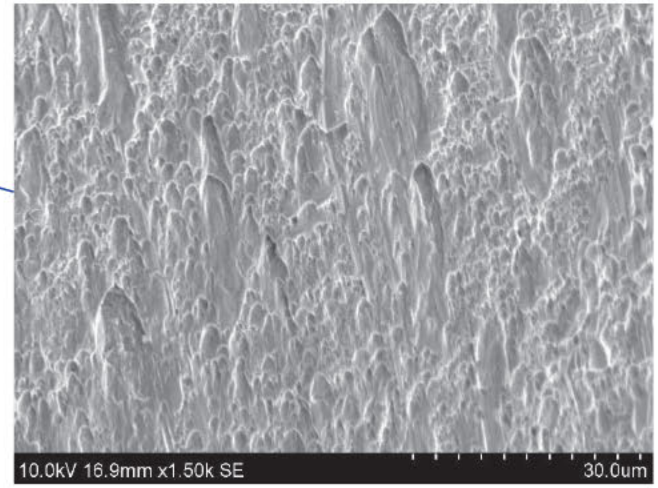

Figure 98. SEM close-up of fracture surface [Bungee Piston]

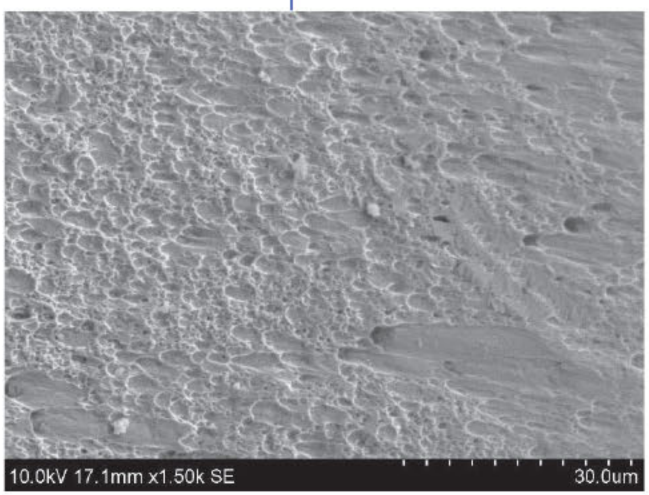

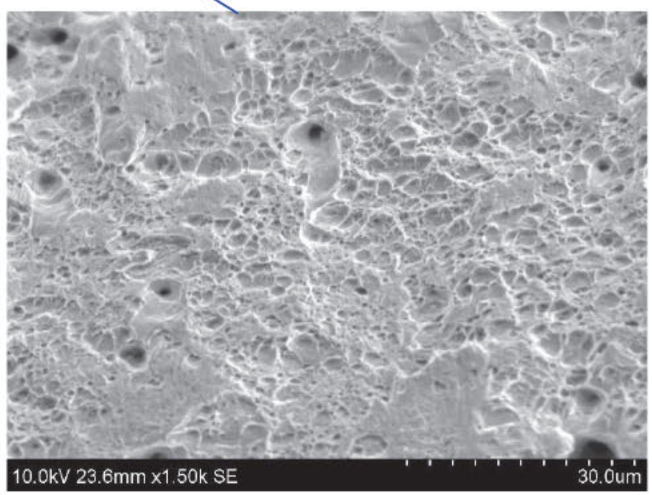

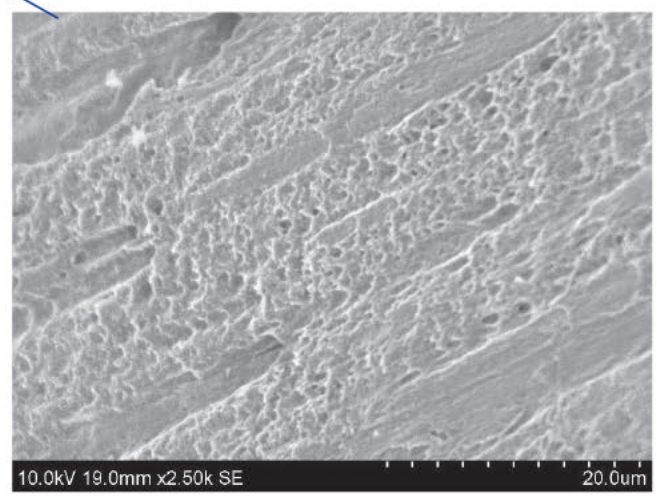

Figures 99 to 101. SEM close-ups of fracture surface [Bungee Piston]

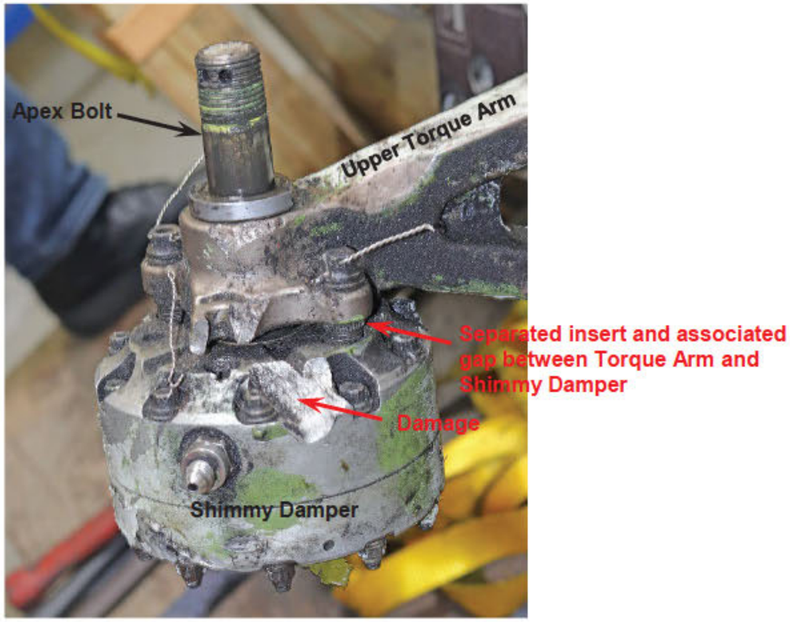

Figure 102. Close-up of Shimmy Damper

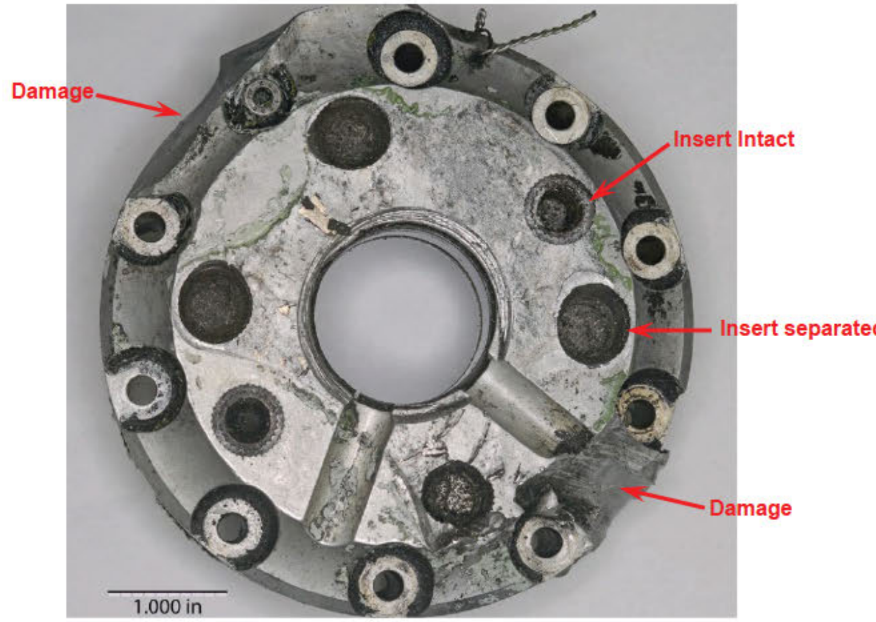

Figure 103. Close-up of Shimmy Damper

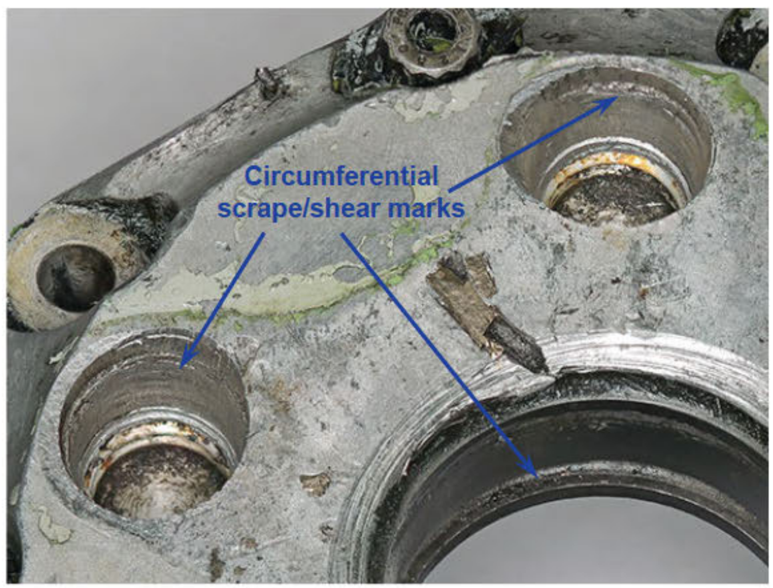

Figure 104. Close-up of holes with no inserts

	Ni	Cr	Mn	Si	Mo	V	Cu	Fe
Lower Torque Arm	1.94	0.81	0.72	2.10 *	0.40	0.07	0.05	Bal
300M Steel (DMS 1935)	1.65 – 2.00	0.70 – 0.95	0.60 – 0.90	1.50 – 1.80	0.30 – 0.45	0.05 – 0.10	≤0.35	Bal

* There may have been a contribution from sanding with silicon carbide to remove CAD layer.

Table I. Chemical analysis of base material by EDS

	Ni	Cr	Mn	Si	Mo	V	Cu	Fe
Lower Side Brace	1.87	0.91	0.88	1.63	0.34	0.09	0.05	Bal
Upper Side Brace	1.86	0.92	0.63	1.82 *	0.42	0.05	0.02	Bal
300M Steel (DMS 1935)	1.65 – 2.00	0.70 – 0.95	0.60 – 0.90	1.50 – 1.80	0.30 – 0.45	0.05 – 0.10	≤0.35	Bal

* There may have been a contribution from sanding with silicon carbide.

Table II. Chemical analysis of base material by EDS

	Ni	Cr	Mn	Si	Mo	Cu	Fe
Retract Rod	1.72	0.90	0.72	0.37 *	0.24	0.21	Bal
4340 Steel (MIL-S-5000)	1.65 – 2.00	0.70 – 0.90	0.65 – 0.85	0.15 – 0.35	0.20 – 0.30	≤0.35	Bal

* There may have been a contribution from sanding with silicon carbide.

Table III. Chemical analysis of base material by EDS

	Ni	Cr	Mn	Si	Mo	Cu	Fe
Lower Lock Link	1.78	0.34	1.41	2.0 *	0.38	0.02	Bal
Hy-Tuf Steel (DMS1841/AMS6425)	1.65 – 2.00	0.20 - 0.40	1.20 – 1.505	1.30 – 1.70	0.35 – 0.45	≤0.35	Bal

* There may have been a contribution from sanding with silicon carbide.

Table IV. Chemical analysis of base material by EDS

	Cr	Ni	Cu	Nb	Mo	Mn	Si	Fe
Bungee Rod	16.37	4.00	3.23	0.37	0.27	0.59	0.90	Bal
17-4 PH CRES (AMS 5643)	15.00 – 17.50	3.00 – 5.00	3.00 – 5.00	5C – 0.45	≤0.50	≤1.00	≤1.00	Bal

Table V. Chemical analysis of base material by EDS

Appendix 1

Evaluate Quality of Red Air Airline MD-82 Left Hand Main Landing Gear Hydraulic Fluid for NTSB Investigation

Requestor: [redacted]

Job Conductors: [redacted]

Date: 08-08-2022

MS 80040

Appendix 1

PURPOSE

On 21 June 2022 at approximately 17:38 local time, a Red Air MD-82, registration HI1064, on flight L5203 experienced a runway excursion and gear collapse during landing on runway 09 at Miami International Airport. Initial reports indicate the left main landing gear collapsed prior to the excursion, and the aircraft subsequently came to rest left of the runway with a fire developing on the right wing after contacting ground equipment.

The lower servicing valve was sheared off, thus the shock strut had no pressure and had lost fluid during the event. Fluid started flowing out of the sheared off valve hole when the gear was removed and laid on it's side, so an empty 16 fl. oz. water bottle was used by to quickly collect some of the fluid.

Approximately 8 fl. oz. of yellow-black MLG hydraulic fluid (S/B DPM 6176) was submitted in an emptied 16 fl. oz. water bottle (Figs. 1-2) for evaluation of the condition (moisture, contamination, etc.) of the fluid.

Appendix 1

PROCEDURE

1. The hydraulic oil was identified using the Nicolet Nexus 4700 Fourier Transform infrared spectrometer with the attenuated total internal reflectance (FTIR-ATR) attachment.

2. The Acidity was measured using an Orion t910 autotitrator per ASTM D664.

3. The Moisture Content was measured per ASTM D6304 using the Mitsubishi CA-06 Karl Fisher titrator with the water vaporizer attachment, since the dialkyldithiophosphate additive in the MIL-5606 base will interfere with the direct injection Karl Fisher titration method. The vaporizer was run at 112 deg. C, with a 3-minute hold and a 300 mL/min dry nitrogen gas flow rate.

4. The oil was filtered with a Millipore filtration apparatus, using a 0.45 micron pore size Durapore filter membrane. Less than 50 mL of oil mostly stopped the filtration so the remaining oil was decanted and the particles were flushed with hexane to remove the hydrocarbon base. The resulting filter was identified as filter 1 (7-25-22).

A second filtration of less than approximately 30 mL did not require decanting excess hydraulic oil and may be a better representation of all particles, including those that may have been suspended. the particles were flushed with hexane. The resulting filter was identified as filter 2 (7-26-22).

4.a. The filtered particles were analyzed using the FTIR-ATR attachment.

4.b. The filters were submitted for SEM-EDS analysis using the Hitachi S-3000N variable pressure Scanning Elecrtron Microscope with Oxford X-Max x-ray analyzer (SEM-EDS).

5. Approximately 7 mL of DPM6176 hydraulic oil was boiled in a 20x175 mm test tube over a Meeker burner for five minutes in an attempt to reproduce the black silting found in the sample.

Appendix 1

RESULTS

1. Hydraulic Fluid was identified by FTIR analysis as DPM6176, MIL-PRF-5606 (Fig. 4) (meets requirements).

2. Acidity = 3.59 mg KOH/g (meets requirement of 2.3-5.0 mg KOH/g)

3. Moisture Content = 772 ppm (fails requirement of $\leq$150 ppm)

Sample was run 4 times:

Run #1 = 721.5 ppm

Run #2 = 777.5 ppm

Run #3 = 767.4 ppm

Run #4 = 823.4 ppm

Average 4 runs = 772 ppm

4. A photograph of the oil before (left Petri dish) and after (right Petri dish) filtering are shown in Figure 2. Based on the dark and light areas of the oil that was filtered, the visual inhomogeneity may be the result of the presence of black, submicron sized particles passing through the 0.45 micron pore size filter.

4a. The filter membranes that trapped the black particles are shown in Figure 3.

The FTIR spectra of the black filtered silt on both filters were similar (Fig. 5). A mixture of Teflon particles, possibly an acrylic material, zinc dialkyldithiophosphate wear additive and residual hydrocarbon oil residue may be present.

Appendix 1

RESULTS (Continued)

4b. SEM-EDS analysis of the black silt identified the presence of fluorine and zinc, sulfur and phosphorus (SEM Figs. 6-9) which are consistent with the presence of Teflon and the hydraulic oil wear additive, respectively.

5. Boiling unused DPM6176 hydraulic oil in a test tube over a burner flame for 5 minutes turned the oil from red to orange but remained clear and did not generate the large amount of particulates found in the sample oil taken from the aircraft.

SUMMARY

The yellow-black hydraulic oil was identified as DPM6176 (MIL-PRF-5606), as required. The oil met the acidity requirement but failed the moisture requirement, possibly due to the sample having been collected in an emptied water bottle that may have had a residual amount of water remaining.

The filtered black silt appeared to consist of a mixture of oil, an acrylate and the wear additive from the hydraulic oil, but the source of Teflon particles (probably from wear) was unknown. It was suspected that the black particles that passed through the 0.45 micron pore size filter were carbon soot, which may also have been a component of the solids that were retained by the filter. Carbon was not identifiable by FTIR analysis. The carbon particles may have been picked up if it flowed over contaminated external surfaces during collection.

The heavy, black silting could not be reproduced by boiling DPM6176 hydraulic oil in a test tube over a burner flame for 5 minutes.

Appendix 1

Red Air MD-82 LH MLG Hydraulic Oil Submitted in Emptied Water Bottle

Figure 1. Hydraulic oil, in water bottle after approximately 75 mL was removed.

Appendix 1

LH MLG Hydraulic Oil Before and After Filtering Through a 0.45 Micron Pore Size Nylon Filter

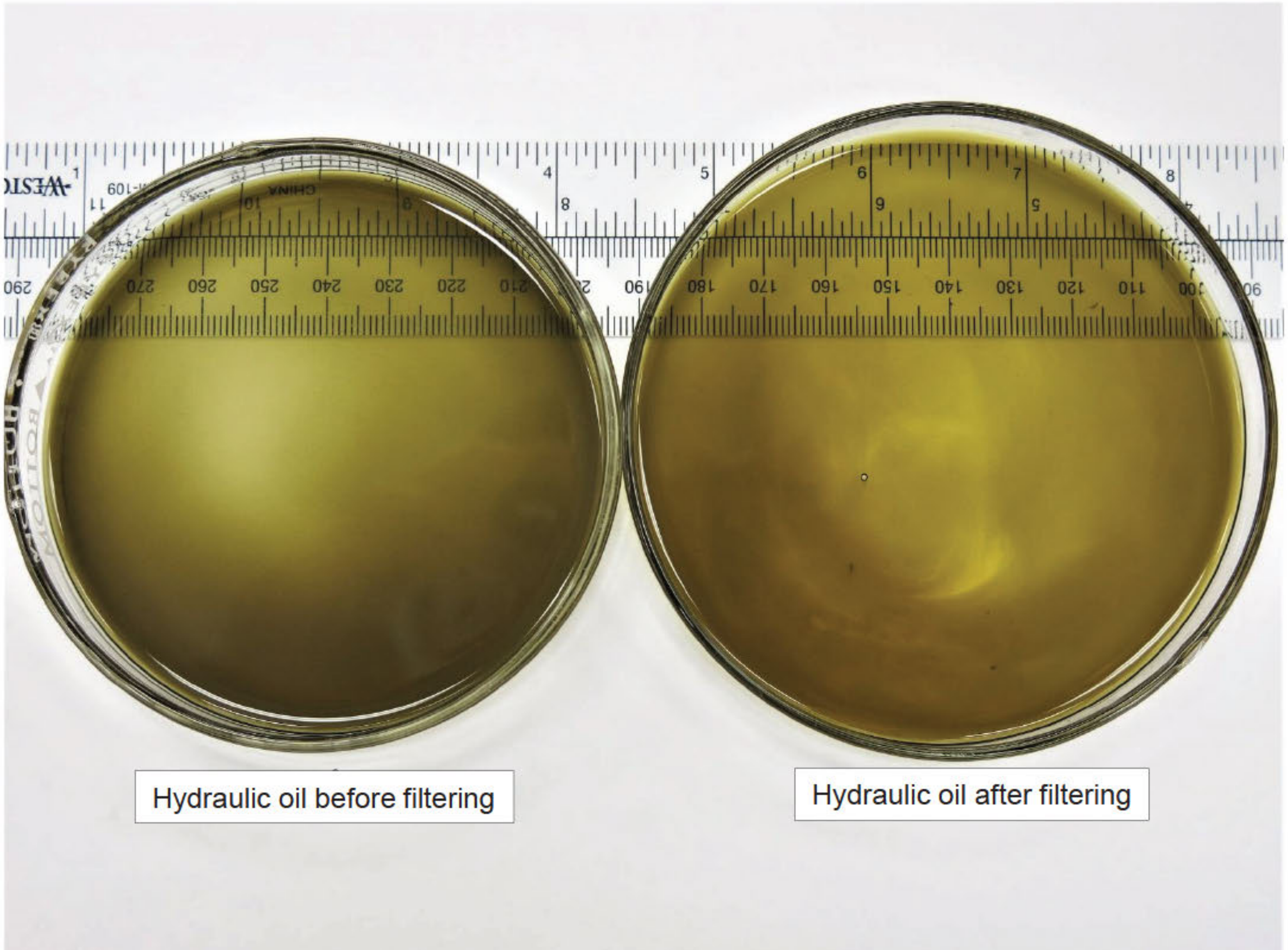

Figure 2. Hydraulic oil, as-received in a Petri dish on left; hydraulic oil after filtering through 0.45 micron pore size filter on right. Particulates still appear to be present in filtered oil.

Appendix 1

Particles Filtered from Red Air MD-82 LH MLG Hydraulic Oil after Removing Samples for FTIR and SEM Analyses

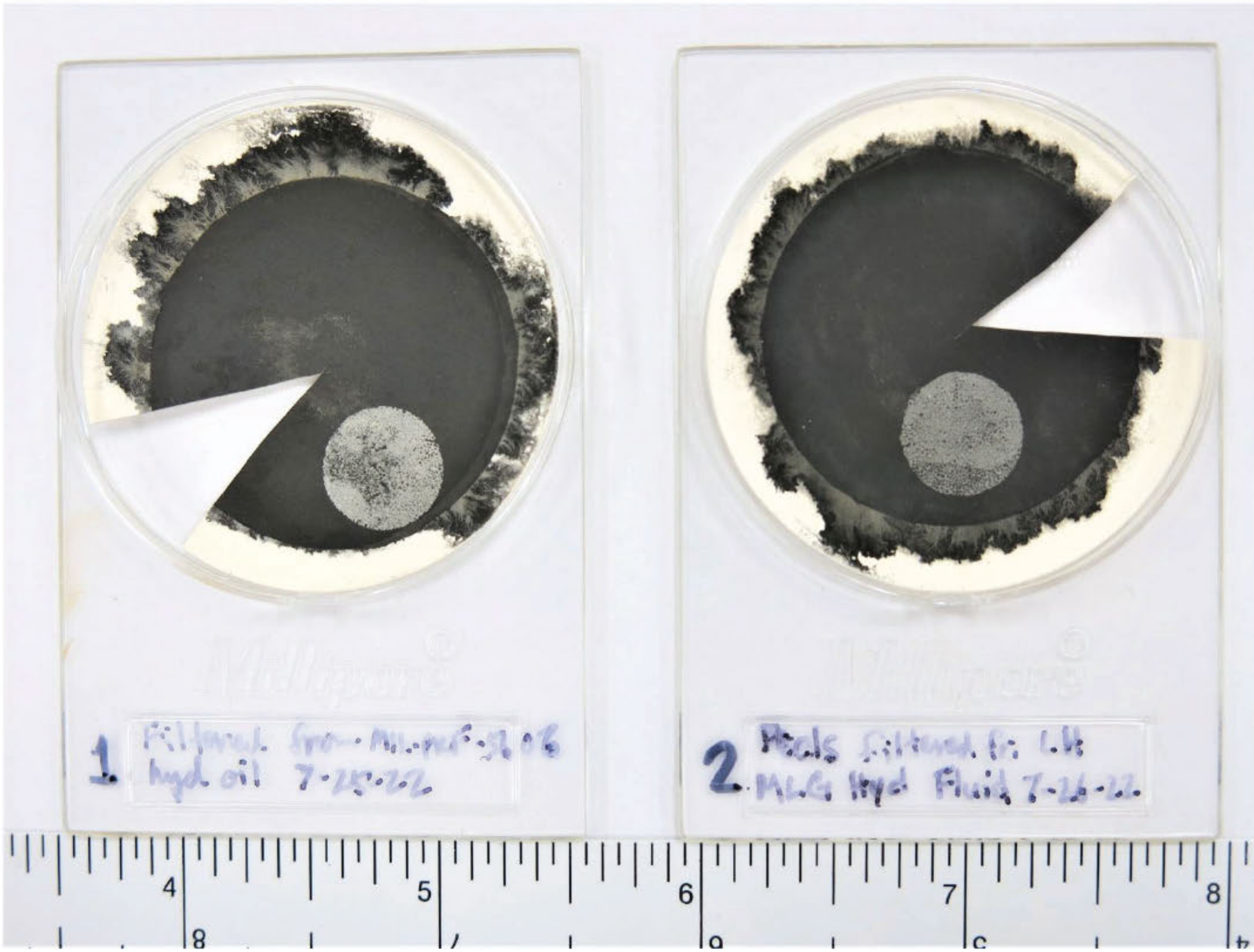

Figure 3. Particles filtered from oil. Filter 1 with particles left after decanting oil after filter plugged. Filter 2 with particles filtered from entire volume of oil added to filter. Both were hexane flushed.

Appendix 1

FTIR Spectrum of Red Air LH MLG Hydraulic Fluid

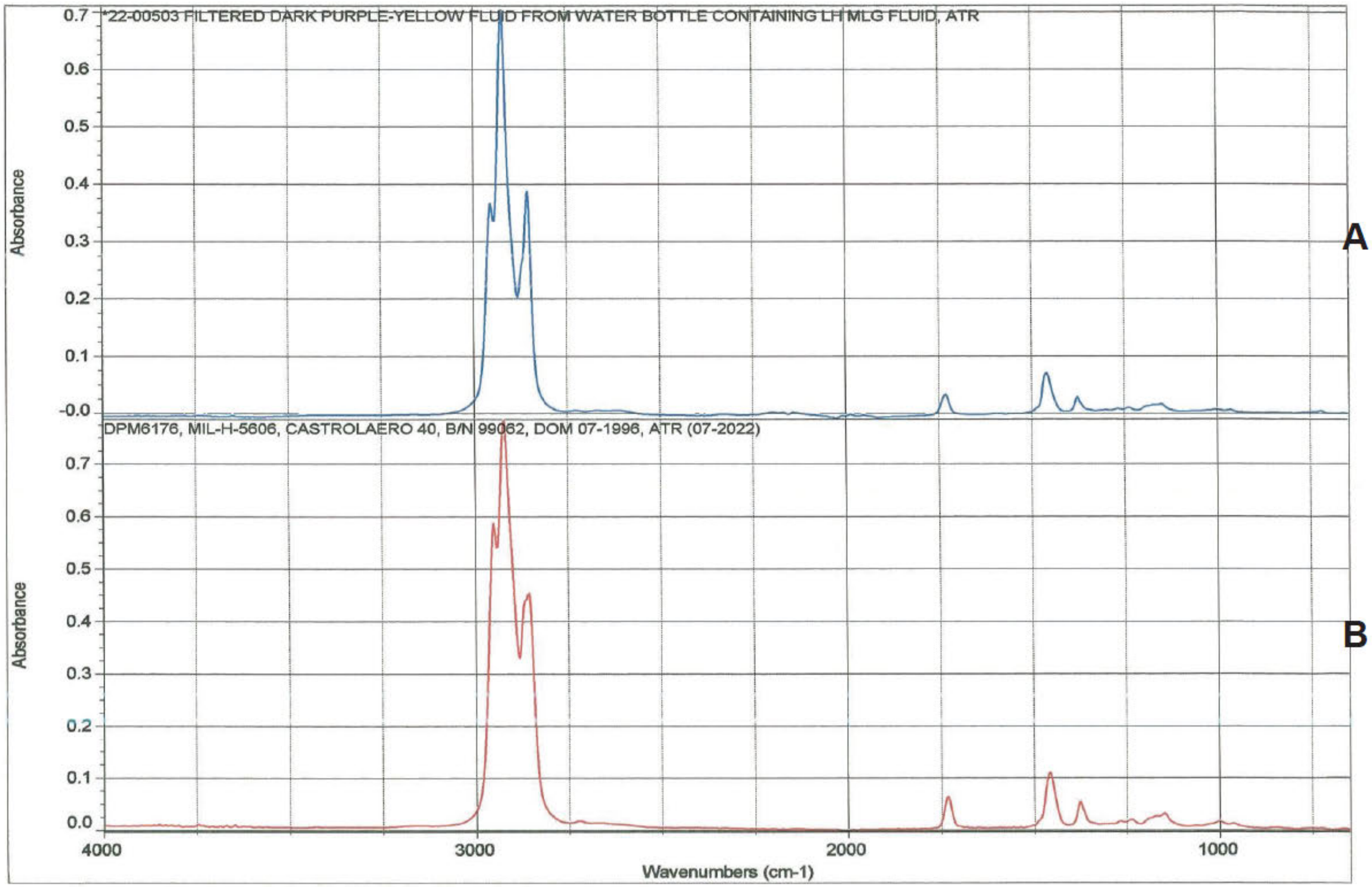

Figure 4. FTIR spectrum of hydraulic oil in blue (A), reference spectrum in red (B).

Appendix 1

FTIR Spectra of Black Particles Filtered from Red Air LH MLG Hydraulic Fluid

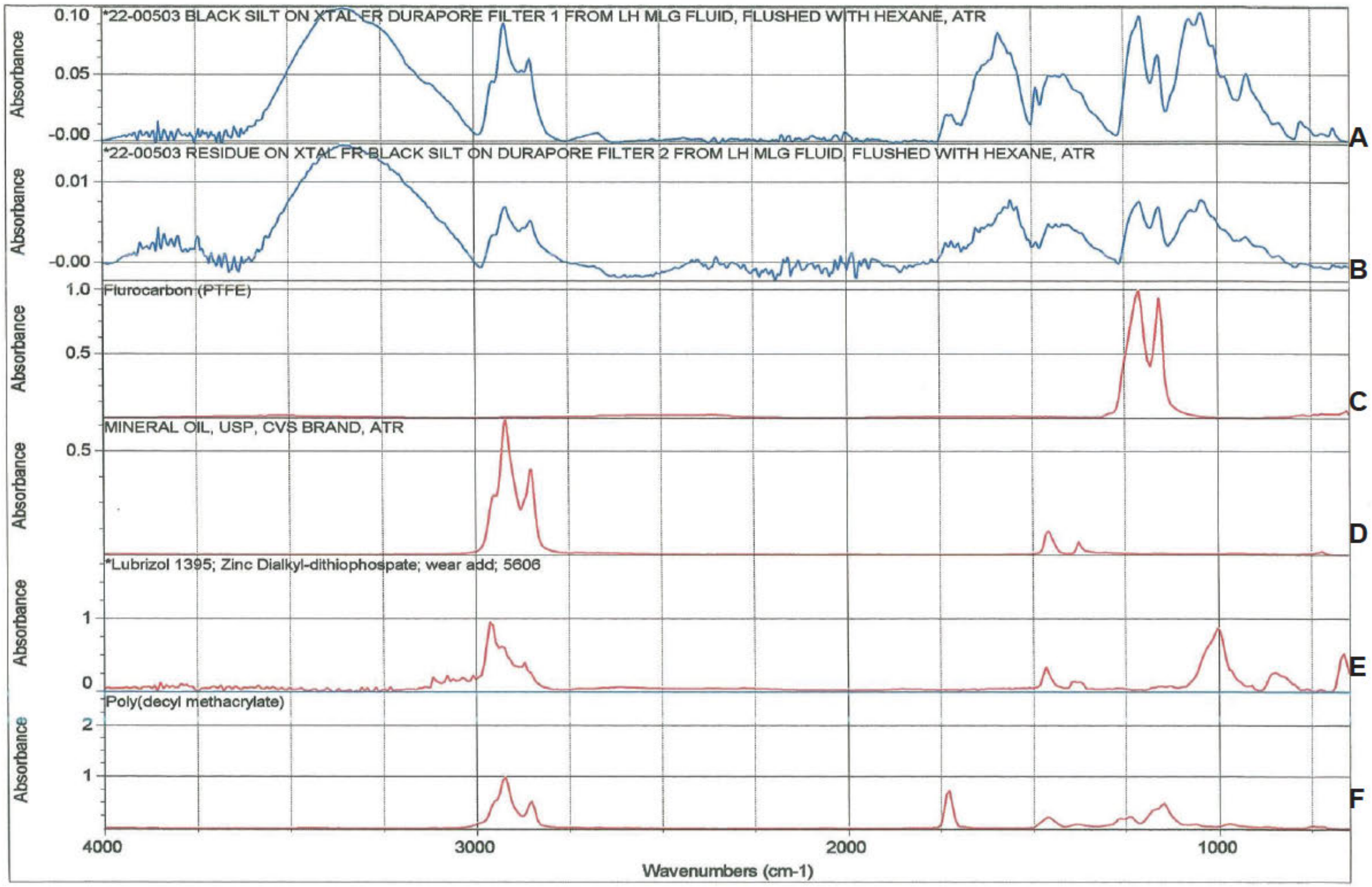

Figure 5. FTIR spectra of filtered black silt in blue (A-B), reference spectra in red (C-F).

Appendix 1

Hydraulic Oil Filter Sample 1 (7-25-22)

Filter material was transferred to carbon tape

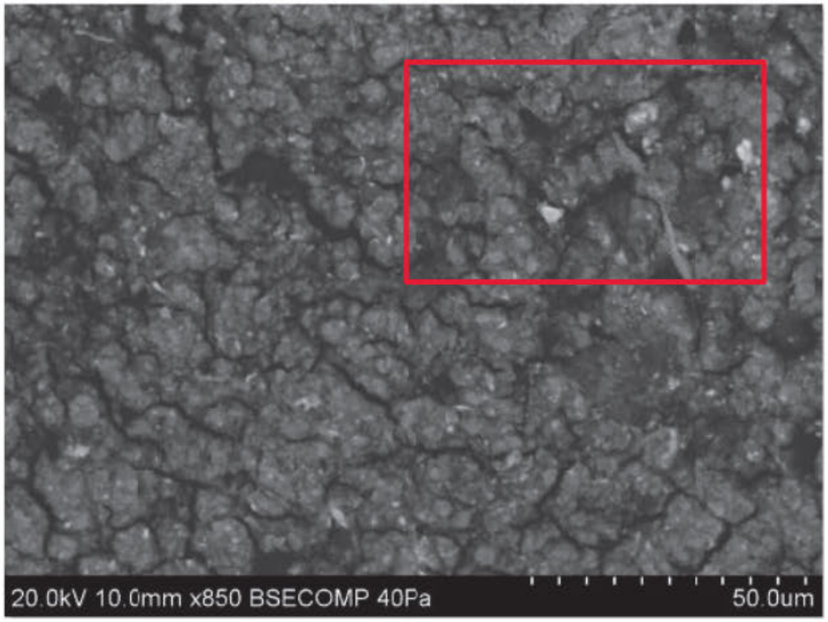

SEM Figure 6. SEM image showing material distribution after transferring to carbon tape.

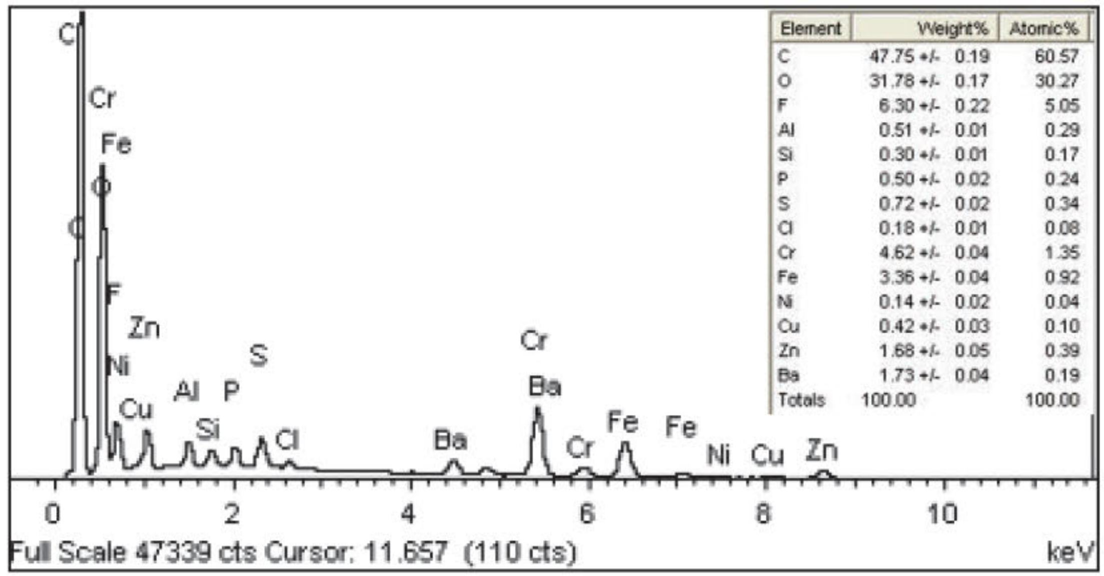

Element	Weight%	Atomic%
C	47.75 +/- 0.19	60.57
O	31.78 +/- 0.17	30.27
F	6.30 +/- 0.22	5.05
Al	0.51 +/- 0.01	0.29
Si	0.30 +/- 0.01	0.17
P	0.50 +/- 0.02	0.24
S	0.72 +/- 0.02	0.34
Cl	0.18 +/- 0.01	0.08
Cr	4.62 +/- 0.04	1.35
Fe	3.36 +/- 0.04	0.92
Ni	0.14 +/- 0.02	0.04
Cu	0.42 +/- 0.03	0.10
Zn	1.68 +/- 0.05	0.39
Ba	1.73 +/- 0.04	0.19
Totals	100.00	100.00

SEM Figure 7. Corresponding EDS spectrum and approximate chemical composition of sample on carbon tape.

Appendix 1

Hydraulic Oil Filter Sample 2 (7-26-22)

Filter material was transferred to carbon tape

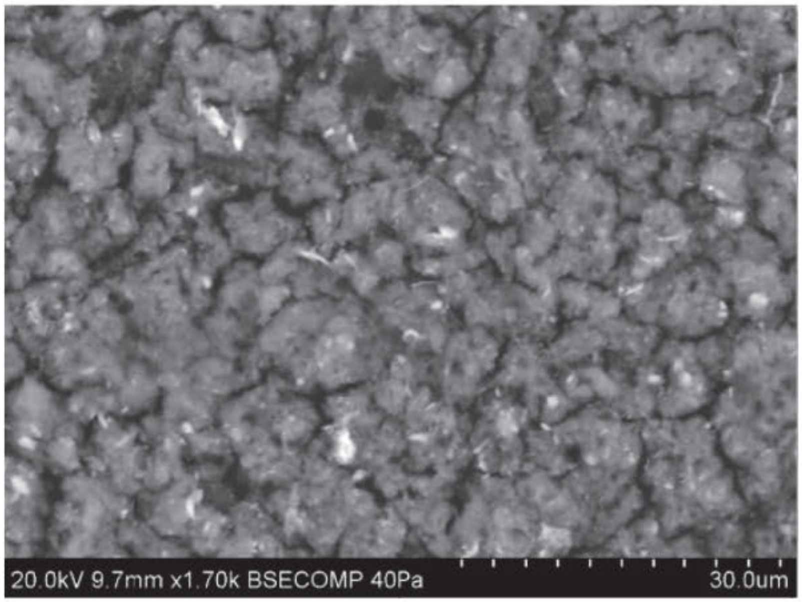

SEM Figure 8. SEM image showing material distribution after transferring to carbon tape.

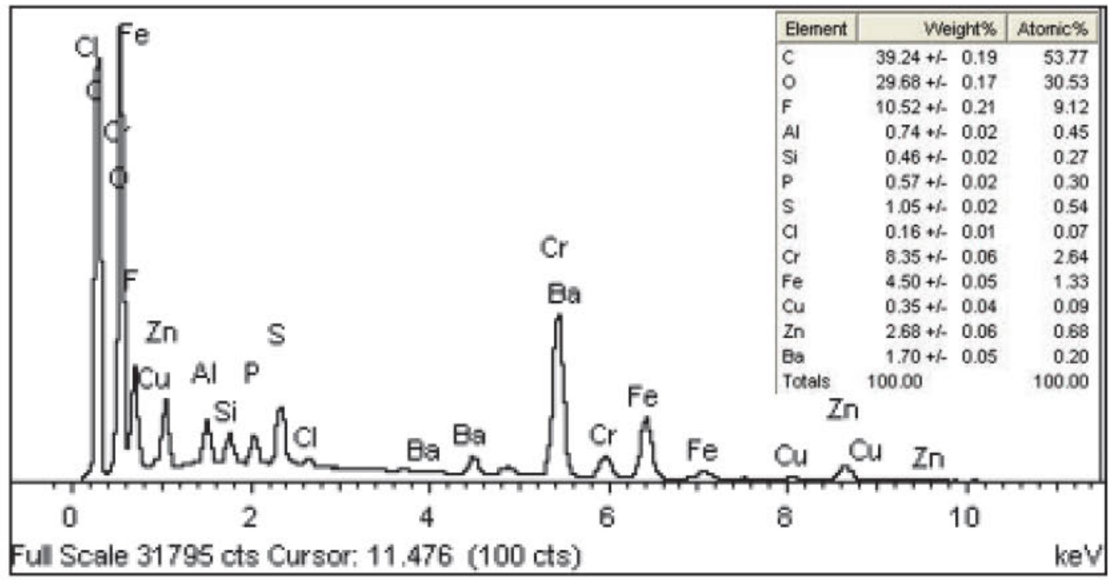

Element	Weight%	Atomic%
C	39.24 +/- 0.19	53.77
O	29.68 +/- 0.17	30.53
F	10.52 +/- 0.21	9.12
Al	0.74 +/- 0.02	0.45
Si	0.46 +/- 0.02	0.27
P	0.57 +/- 0.02	0.30
S	1.05 +/- 0.02	0.54
Cl	0.16 +/- 0.01	0.07
Cr	8.35 +/- 0.06	2.64
Fe	4.50 +/- 0.05	1.33
Cu	0.35 +/- 0.04	0.09
Zn	2.68 +/- 0.06	0.68
Ba	1.70 +/- 0.05	0.20
Totals	100.00	100.00

SEM Figure 9. Corresponding EDS spectrum and approximate chemical composition of sample on carbon tape.

APPENDIX 2 - MS 80040

Red Air MD-82 HI1064 – LH Main Landing Gear and Shimmy Damper Test Plan

1. Document and photos of the contents of the received crate / shipments.
    a. Note and photo any discrepancies (for example: lower servicing valve sheared off from cylinder)
2. Measure gap at the torque arm apex.
3. Measure gap / axial freeplay where the lower torque arm attaches to the piston.
4. Measure gap / axial freeplay where the upper torque arm attaches to the cylinder.
5. Disassemble / remove the lower torque link segment from the piston.
6. Disassemble / remove the upper torque link and attached pieces from the outer cylinder.
7. After removing the torque links from the shimmy damper, X-Ray inspect the shimmy damper. The intention is to determine the build-up and orientation of internal parts.
8. Dimensional check as shown on figures
9. Fracture analysis on the following:
    a. Upper Torque Arm
    b. Lower Torque Arm
    c. Upper Side Brace
    d. Lower Side Brace
    e. Lower Lock Link
    f. The sheared portion (threaded boss) of the damper reservoir (or the mating portion lodged in the damper housing)
10. Disassemble the shimmy damper, keeping careful attention on the orientation of the internal parts. The shimmy damper has qty 10 belleville washers that are supposed to be installed in a defined orientation.
    a. Via part number and part examination, verify the following service bulletins have been incorporated in the received shimmy damper
        i. SB-MD-80-32A275
        ii. SB-DC9-32-311
        iii. MD80-32-278
11. Chemical analysis of Landing Gear fluid sample.

Lab actions and findings

Boeing Metallurgical Lab

Huntington Beach, CA

19 July 2022

Photographed and documented as-received crate.

- Initial observation was that the landing gear shifted during shipping, due to a wooden cradle supporting one of the axles collapsed. However, not damage noted to the landing gear due to this.

Several gap dimensions taken with the landing gear assembled; See dimensional inspection sheet.

Shimmy Damper

- A large gouge was noted in the shimmy damper housing.
- Of the four (4) bolts attaching the damper to the upper torque arm, one bolt was missing, with the torque arm lug sheared, and lockwire sheared.
- Of the three (3) remaining bolts, they were loose with the threaded inserts pulled out (but still present) from the damper housing.

Torque Arm Apex joint

- The Hydraulic support bracket freely rotates.
- A gap found between the lower torque arm lug and nut (approx. 1/8 to 3/16 inch).
- The Hydraulic support bracket was bent.
- The washer was not flat (normal) but was coned with wear marks on each side.
- A bushing flange was sheared/missing.
- Stop was damage on the Outside diameter, but had the full circumference.
- Another bushing flange was sheared fully around its entire circumference but intact.
- The lower torque arm lug was sheared in half, with half of the lug remaining in the apex joint.

Disassembled the torque arm apex joint and removed shimmy damper housing. The torque arm apex bolt was stuck in the damper housing. Visual inspection noted that the bolt was bent. Attempted to use a hydraulic press to remove the bolt form the housing, but unable to (stopped out of concern of damaging housing.

- After discussion with the NDT technician, decided to forgo X-ray inspection of the housing assembly. This was due to the steel bolt inside the Al Housing would not yield clear/desired results.

Proceeded to disassemble the housing assembly from one end, with the bolt stuck. The internal components were found to be assembled correctly. Of note was finding few small metallic particles/debris.

- Measured and recorded the break-away torque of the 10 housing attach bolts.

20 July 2022

Shimmy Damper

- The stuck torque arm apex bolt was cut to enable removal from the damper housing, and thus allow for the remaining half of the disassembly to occur.
- The internal components were found assembled correctly.
- On recovered damper nameplate (damaged and recovered with the reservoir pieces) was vibroetched SR09320057-7009, S/N DL84, DAM5705

Laid out the Side Braces segments

- Evidence of damage originally thought to forward side was actually the aft side.
- When laid out on the cylinder, the side brace damage aligned with damage on the outer cylinder (fwd side, near the gland nut end).
- Contact damage at the upper/lower side brace joint, along with the damage described above, indicates the side braces “hyperextended” or folded in opposite direction than normal.
- There was also segment of tire rubber imbedded in the joint; the tire likely in the path of the side braces folding in the opposite direction.

Lower lock link (P/N 5935350-7, S/N CPT0893) was bent and sheared; the bend is in the aft direction.

Witness (contact) marks on / between upper lock link and cylinder.

Bungee cylinder – rod end sheared off, and witness mark between rod end and outer cylinder.

21 July 2022

Performed dimensional inspections (See dimensional inspection spreadsheet (Appendix 3)).

Shimmy Damper orifice dimensions taken.

Check valve removed from shimmy damper; break-away torque measured 250 in-Lbs.

Landing Gear

- Removed additional components including bungee cylinder and its' bracket.
- Witness marks (contact) on hydraulic pipes (outboard side, most fwd and most aft); impact/out of round at end near out cylinder.
- A mark on the outer cylinder where the otbd/fwd pipe contacted.
- Witness mark on outer cylinder aft trunnion lug, outboard side; base metal visible.
- Witness mark on outer cylinder, outbd side just aft of fwd trunnion lug; base metal visible.
- Retract actuator piston complete fracture. Piston end still attached to outer cylinder, and bends inward to cylinder.
- Downlock springs in-tact / no damage.
- Lower servicing valve sheared; flush with outer cylinder

Upper side brace – mid way lower side has impact/witness mark opposite of fracture.

27 July 2022

Completed dimensional inspections.

Some freeplay noted between the bracket and upper lock link, so performed dimensional checks and added to spreadsheet.

Damper Mounting Bolts

- 3 of 4 remain attached to the upper torque arm with inserts still attached; i.e. inserts pulled out of the damper housing
- Checked gap / freeplay of the 3 bolts (between torque arm face and insert)
    - 0.039B
    - 0.031
    - Tight, 0.0

Lock Links

- Lower lock link – small segment missing (approx. 3/16”) between fracture faces.
  Bent up and aft
- Upper lock link – bent forward
  - Damage on aft side of the prox sensor target area.

Side Braces

Discussed metallurgical analysis findings.

- One pre-existing condition (internal granular features) on the lower side brace
- One I.G. / quasi-cleavage area on the upper side brace.

Based on the other damage areas found on the side braces, it was determined that these areas of I.G. findings did not result in fracture either of the side braces. Each side brace (upper and lower) was fully intact and connected when the side brace assembly hyper-extended, when the side braces contacted the outer cylinder, and leaving the damage markings. Thus, it was determined that both side braces fractured when they contacted the outer cylinder, and not due to any pre-existing conditions.

Torque Arms

Laid out the torque arms, along with the fractured portion of the lower lock link lug. Visual inspection found that the fractured lower torque arm lug bent inboard (permanent deformation before fracture). This is consistent with the metallurgical fracture analysis regarding the shear direction.

28 July 2022

Damper Housing

Re-examined the damper housing, with more detail on the attach holes (where the mounting bolts/inserts pulled out). All 4 holes missing inserts and smooth bore. 3 of the holes are oversized and oblonged in varying direction, and follow the circumference of the housing. The elongation was at the outer depth of the hole; the inner depth was round. The inner depth (bottom of hole) had few threads intact / not smeared (these are the threads the insert would thread into).

It was observed that a paint pattern on the housing was consistent with the outline of the upper torque arm mounting area, indicating the housing had paint (grey) applied after it was installed onto the torque arm (which is not as expected).

Torque Arm Apex Bolt

The hardness of the torque arm apex bolt was measured; HRc = 41. This is consistent with the expected hardness (HRc 40 to 43) for this bolt (HT = 180 to 200 KSI).

Appendix 3

Red Air MD-82 HI1064 – LH Main Landing Gear - Dimensional Check

As assembled, gap at the torque arm apex = 0.330 and 0.348

As assembled, gap / axial freeplay between lower torque arm and piston = 0.014

As assembled, gap / axial freeplay between upper torque arm and cylinder = 0.025

Part Name	Part Number	Feature	Design Dimension	Measured Dimension	Comments
Upper Torque Arm	5935374-1	Lug Span, bushing face-to-face	5.6152 / 5.6260	5.662 / 5.668	
	5935374-5	Lug Bore diameter (I.D.)	diameter 2.000 / 2.001	INBD 2.002/2.011 OUTBD 2.020/2.002	with bushing
	S/N MAL112	Lug width, with bushings	1.6888 / 1.6760	1.198	bushing flanges partially missing one each side. Measured and max. thickness
		Lug Bore diameter (I.D.)	diameter 1.187 / 1.188	INBD 1.192 OUTBD 1.192	with bushing
Lower Torque Arm	5935353-1	Lug width, with bushings	6.1978 / 6.1890	6.19	
	5935353-5	Lug Bore diameter (I.D.)	diameter 1.875 / 1.87	1.1875 / 1.1875	with bushings
	S/N MAL294	Lug width, with bushings	1.2458 / 1.2370	not measured	one side shoulder bushing flanges sheared off
		Lug Bore diameter (I.D.)	diameter 1.187 / 1.188	not measured	tight fit w/ sleeve. Sleeve I.D. 1.001
Cylinder	5935348-503	Lower Lug width, with bushings	5.6128 / 5.6040	5.615 5.630	bushing faces no parallel
		Lug Bore diameter (I.D.)	diameter 2.000 / 2.001	fwd-aft 2.012 up-dn 2.022	ovalized, same both sides
Piston	5935347-507	Lower Lug Span, bushing face-to-face	6.2080 / 6.1992	6.206	
		Lug Bore diameter (I.D.)	diameter 1.8760 / 1.8750	1.876 1.875	
Torque Arm Apex Bolt	4925624-505	Shank diamter (O.D.)	diameter 0.9990 / 0.9980	not measured	bent and stuck in damper housing
4925624-501 "PBF"	S/N CPT979	Length, shank + threads	5.226 / 5.216	not measured	6.234 head to end hardness checked = 41 HRc
Torque Arm Apex Spacer	4692620-1	Thickness	0.307 / 0.317	0.308 0.307	
Torque Arm Apex Spacer	2923128-503	Length	2.102 / 2.098	2.15	
Torque Arm Apex Stop	2923122-1	Thickness	0.279 / 0.283	0.278 0.274	damage on O.D.
Torque Arm Apex Spacer	4923134-501	Length	1.255 / 1.251	1.253	
Washer	AN960C1616	Thickness	0.090 +/- .008	0.083 0.063 in groove	groove not entire circumference
Washer	4D0053-16P32-8	Thickness	0.078 +/- .007		N/A above washer installed
Hydr Support Bracket	7936911-565	Thickness	0.125	0.125	
Lower Lock Link	5935350-501	Lug Bore Diameter (I.D.) 2 PL	diameter 0.6245 / 0.6255	fwd 0.625 aft 0.6255	
5935350-7		Lug Bore Diameter (I.D.)	diameter 2.125 / 2.126	2.139 2.125	ovalized
S/N CPT0893 MHB					
Upper Lock Link	5935349-1	Lug Bore Diameter (I.D.)	diameter 0.561 / 0.562	0.564	
5935349-9		Lug Bore Diameter (I.D.)	diameter 0.6245 / 0.6255	0.6315	
S/N AML0050		Lug Bore Diameter (I.D.)	diameter 0.5015 / 0.5005	0.499	sleeve (O.D. .498) pressed out. I.D. 0.314
		Lug Bore Diameter (I.D.)	diameter 0.8745 / 0.8755	0.8754	
Washer	MS20002C6	Thickness	0.078	0.089	
Bolt	MS21250H06008	Length, shank + threads	1.145	1.146	
Bracket Assy, Bungee	5937032	Lug span, face to face	2.009 +/- .005	2.002	
		Lug Bore Diameter (I.D.)	diameter 0.4995 / 0.5005	0.502 both sides	
Bushing	S2210370P5-30	O.D.		0.498 0.497	
		I.D.		0.314 0.316	